An improved Umkehr algorithm.

I. Petropavlovskikh[1], P. K. Bhartia[2], J. DeLuisi[1]

Abstract. Several improvements have been made to the operational (ca. 1992) Umkehr ozone profile retrieval algorithm by Mateer and DeLuisi (UMK92) and are described here. A key change is in the construction of the a priori profile. In the UMK92 algorithm the a priori profiles are constructed using total ozone column measured by the same instrument. Therefore, UMK92 has the undesirable property that the a priori profiles vary with day and year. These variations make it difficult to ascertain whether the retrieved long-term changes are forced by a priori or whether they reflect information contained in the measurements. In this paper we describe an updated algorithm that uses fixed a priori profiles, which vary with season and latitude, but have no day-to-day or long-term variability. Our new updated algorithm (UMKV8) also has an improved forward model. The informational content of Umkehr measurements is analyzed using the Averaging Kernel (AK) method developed by Rodgers. The UMK92 algorithm employs a normalization procedure that varies based on the availability of the highest solar zenith angle (SZA) measurement. The UMKV8 algorithm is designed to normalize Umkehr measurements to a 70-degree SZA, thus removing seasonal dependence in the normalization procedure. Because the SZA at middle and high latitudes changes slowly with the time, this 70-degree normalization also allows significantly reduces the observation time. Based on AK analysis of the informational content available from the UMKV8 algorithm, we recommend using an 8-layer scheme where ozone is combined in layers 0 and 1, and layers 2 and 3 to represent tropospheric and lower stratospheric changes respectively. We find that ozone information in layer 4 has similar informational content to ozone in layers 5 through 8. Thus, layers 4 through 8 should to be treated as individual layers containing prevalently independent stratospheric ozone information. Layer 9 and above has no independent information but could be combined with layer 8 to get accurate ozone column above 4 hPa; this estimate is important for comparing satellite and ground -based ozone retrievals. Although this technique is too noisy to monitor short-term variability in atmospheric ozone, it is capable of monitoring long-term changes in monthly mean ozone in seven or eight layers with reasonably uncorrelated errors and with minimal influence from a priori information.

1. Introduction

The Umkehr method offers an inexpensive and important international addition to the array of methods used to study ozone profiles and stratospheric ozone trends. The method has served exceptionally well for validating satellite observations, which in earlier years were seen to drift significantly, and has been applied to both ground-based Dobson and Brewer measurements. The retrieval techniques applied to satellite measurements share many common features with the Umkehr method, and have similar vertical resolution and altitude

[1] Cooperative Institute for Research in Environmental Sciences, U. of Colorado, CO 80303, USA

[2] NASA Goddard Space Flight Center, Greenbelt, MD 20771 USA

coverage. For example, Elansky et al. [1999] proposed to utilize the spectral scan of the Brewer's zenith sky radiance measurements to retrieve the ozone profile using a technique similar to the satellite backscatter ultraviolet (BUV) method. The similarity in the physical principles of the ground-based and satellite radiance measurements make the two systems ideal for comparison.

The classical Umkehr curve was first observed at the beginning of the 20th century in the study of total ozone column variations with season and latitude [Dobson, 1930, 1957; Götz, 1931, 1934; Dütsch, 1957, 1959]. Once the photochemical theory of ozone formation in the upper atmosphere was advanced [Chapman, 1930], the vertical distribution of ozone was related to the Umkehr curve.. The curve represents the ratio of zenith sky intensities measured at two wavelengths -- where one has stronger absorption characteristics relative to the other -- as function of solar zenith angle (SZA). The maximum in the ozone profile is clearly detected by inverting the relation between wavelength ratio measurement and solar zenith angle when the sun passes the 85-degree angle. Mateer and Dutch [1964] developed the first computerized version (UMK64) of the algorithm for retrieving the vertical ozone distribution. Two decades later, improved ozone absorption coefficients were published by Bass and Paur [1985] and a new mathematical method for the inversion procedure (the optimal estimation method by Rodgers [1976]) prompted work to update the Umkehr ozone profile retrieval algorithm. A new algorithm (UMK92) was developed by Mateer and DeLuisi [1992] and is currently used operationally at the World Meteorological Organization World Ozone Data Centre (WMO-WO3DC) in Toronto, Canada.

The ozone profile time-series retrieved from the Umkehr measurements are routinely published in so-called "red books" and are also available electronically. The data have been used to intercompare and validate the ozone profile information derived from remote-sensing and in-situ measurements [SPARC Report, 1999; Newchurch et al, 1998; McPeters et al, 1996; etc.]. Recently, Dütch and Staehelin [1992] and Mateer et al. [1996] compared Umkehr retrievals against ozone-sonde data, while Newchurch et al. [1998] compared UMK64 and UMK92 retrievals with Stratospheric Aerosol and Gas Experiment (SAGE) data. Both papers agreed that the UMK92 a priori information in the lower layers was biased to the total ozone and did not reflect systematic anthropogenic changes in the ozone profile. Thus, when the UMK92 retrievals are used for trend analysis, the interference of the a priori information biases the trend detected in the tropospheric ozone to the total ozone trend [Dütch and Staehelin, 1992; Mateer et al, 1996; Petropavlovskikh et al, 2000]. Above the troposphere, in layers 4 through 8, UMK92 was found to provide reliable information for trend analysis. An independent study by Miller [1996] supported this conclusion, but in all layers, variations in the a priori information can make it difficult to ascertain whether the retrieved long-term changes are forced by a priori or whether they reflect information contained in the measurements. To study the true inter-annual variability in the data, the effect of the a priori information on the retrieval should be eliminated.

Assessing changes or trends in the ozone profile requires improved retrievals showing no bias to a priori information. Upper-stratospheric ozone trends have been derived from the Umkehr data and other remote-sensing and balloon measurements [Newchurch et al., 2000; DeLuisi et al., 1994; Mateer et al, 1996; Reinsel et al, 1999; Randel et al, 1999, Miller et al, 1996]. Reinsel et al. [1999] updated the Umkehr ozone profile trend analysis for northern latitude records from 1977 through 1997 and reported a significant ozone depletion trend of –0.5 % per year in layers 7, 8, and combined layer 8 and above. Strong seasonal and latitude dependences were noticed in the trends derived for layers 2 and 3 (Reinsel et al., 1999). Newchurch et al. [2000] found strong

similarities in the amplitudes of the annual variation and trends measured by SAGE I and II and Solar Backscatter Ultraviolet (SBUV and SBUV/2) satellites, and the Dobson network between 1978 and 1998, providing high confidence in the accuracy of the results for upper-stratospheric ozone depletion rates.

According to recent general circulation model (GCM) projections [Shindell, 2002], ozone recovery is most likely to be detected in the middle stratosphere at around 40-km altitude. In this region, pure homogeneous chlorofluorocarbon chemistry is the prevailing factor in ozone destruction; in the lower and upper stratosphere additional processes, for instance changes in temperature or water vapor, may significantly contribute to ozone changes. The Umkehr measurements, along with satellite and lidar measurements have very solid information about ozone variability in this 40-km region, above the altitudes typically reached by ozonesondes. The satellite measurements begun in the 1980s are often limited by problems combining measurements from different instruments to provide a blended ozone record for trend analysis, while lidar measurements are very sparse and often have less than a 15-year record. The long historical record of Umkehr measurements can therefore provide valuable information about ozone loss rates as well as ozone recovery at the important 40-km altitude level. Shindell [2002] also emphasized that there might be different ozone loss/recovery rates found at different latitudes. Thus, ozone trends derived from Umkehr records at the middle latitudes can be compared with results for tropical regions to validate the detection of ozone recovery.

This paper examines improvements and resulting error analyses for the Umkehr ozone profile retrievals. The results should greatly advance the usefulness of the Umkehr data for ozone trend analysis. The improvements to the retrieval algorithm account for all aspects of the observations and theory, from instrumentation (described in Section 2.1), to the forward model (Section 2.2) and inverse model (Section 2.3). Section 3 discusses the analysis of synthetic data, and Section 4 provides information on errors. Sections 5 illustrate the algorithm's ability to retrieve a profile and a test trend respectively, and Section 6 presents an overview of the new algorithm's features.

2. Background.

2.1. Instrument description.

The Dobson and Brewer instruments report zenith-sky measurements in terms of N-values, mathematically represented as:

$$N(\theta) = 100 \times \log\left(\frac{F_0' \times K' \times C'}{F_0 \times K \times C}\right) \qquad (1a)$$

where F_0 is the extraterrestrial solar flux constant, K is the instrumental constant, and C and C' are the photon counts related to zenith-sky intensities I and I' (ZSI) at two wavelengths, where the prime denotes the longer wavelength. The observations are made as SZA, θ, changes from 60^0 to 90^0. Umkehr observations are made by several Zenith-sky UV (ZUV) instruments currently employed around the world. There are three known techniques currently employed. The standard (manual) Dobson measurements are taken at the single C-pair wavelength (311.4 and 332.4-nm) as SZA, θ, changes from 60^0 to 90^0. Traditionally, Umkehr measurements are

reported at 12 nominal SZAs (60, 65, 70, 74, 77, 80, 83, 85, 86.5, 88, 89, and 90 degrees). The automated Dobson measurements are taken at a higher rate than the standard, manual Dobson measurements. In addition to C-pair measurements, the automated Dobson instrument employs zenith-sky measurements at two additional wavelength pairs (A- and D-pairs consisting of 305.5/325.4-nm wavelengths and 317.6/339.8-nm wavelengths, respectively). The Brewer technique is similar to the automated Dobson, however the central wavelengths and width of the band paths are chosen differently. The wavelength details for the Dobson instrument can be found in Komhyr [1980, 1989] and Mateer [1964]; those for the Brewer are reported by McElroy et al [1995] and WMO [1998b, 1998d].

None of the instruments is calibrated in zenith sky radiance mode. Therefore, the instrumental constants (K and K′) are unknown. In addition, atmospheric parameters (F_0 and F'_0) are not known accurately. There are also known episodes of instrument exchange and repairs of the optical parts, and calibration shifts have also been detected (Petropavlovskikh et al. [2001]). Because of these factors, a normalization procedure is used to cancel out the unknown parameters. Most typically, a measurement at the highest sun elevation (usually at 60-degrees SZA) is subtracted from measurements at other nominal SZAs:

$$y(\theta) = N(\theta) - N(\theta_0), \qquad (1b)$$

where $y(\theta)$ is normalized measurement, N is Umkehr measurement, θ is one of nominal SZAs, and θ_0 is the normalization SZA. This process reduces the measurement to that of the diffuse sky transmittance.

The procedure assumes that the instrumental parameter does not change with SZA. Therefore, subtracting the measurement at 60-degrees SZA from the measurements at other SZAs makes the retrieval insensitive to calibration and solar flux uncertainties, and the technique can be described as “self-calibrating”, similar to solar-occultation techniques from space (such as SAGE, GOME, etc.). We later (see Section 6.1) show that the normalization technique also makes the measurements essentially insensitive to tropospheric aerosols and surface albedo. During wintertime at high latitudes where the sun does not reach a 60^0 SZA, the measurements at 70º, 74° or 77º SZA can be used for normalization.

Umkehr observations are accompanied by direct-sun total ozone measurement providing critical information for the profile retrieval algorithm. The total column ozone is determined by direct-sun measurements taken at the AD-pair wavelengths (AD is a double pair consisting of A and D pair wavelengths). Typically, the total ozone measurements are not taken at the same SZAs as the zenith-sky measurements. Therefore, the variation in total ozone, as well as in other atmospheric parameters (cloud cover and aerosols) during the Umkehr measurement can introduce uncertainties in the retrieved ozone profiles (see Section 4.1).

2.2. Forward model.

The forward model is used to describe the relation between an ozone profile distribution and an Umkehr N-value. In order to use the forward model we need to know how the N-values depend on ozone, aerosols, surface reflection, air refraction, and multiple-scattering assumptions. The model requires information on ozone absorption and Rayleigh scattering cross-sections for the UV-part of solar spectrum where Dobson measurements are taken. For the retrieval algorithm it allows us to calculate partial derivatives (or weighting functions) that provide information about sensitivity of N-values with respect to ozone profile. The updates to the forward model include improved standard ozone profiles; updated multiple-scattering corrections for N-values;

updated refraction and temperature correction for N-values; tabulated multiple-scattering corrections for Jacobian; updated spectroscopic data such as ozone absorption, Rayleigh cross-sections, extraterrestrial solar flux data, as well as generalized C-pair Dobson slit functions. Information inAppendix A details the forward model set-up.

2.3. Inverse Model.

The inverse method uses a maximum likelihood estimation procedure and is based on Rodgers [2000, and therein], including the UMK92 retrieval method [Mateer and DeLuisi, 1992]. The most important changes to the inverse model of the new UMKV8 algorithm include the following: the ozone profile retrieval is done at higher resolution (using quarters of Umkehr layers), which is consistent with the vertical resolution of the forward model, and effectively eliminates interpolation errors embedded in the UMK92 code; the a priori covariance matrix is modified according to recommendation by Rodgers [2000] (see further discussion in Sections 3 and 4); the error covariance matrix has solar zenith angle dependence as compared to the angle-independent error matrix in the Umk92 algorithm; and the weighting function is linear in ozone amount (which improves probability distribution function) as compared to a log-scale approach in the Umk92 retrieval. In Appendix B we provide detailed information regarding changes made to the inverse model of the UMKV8 algorithm.

3. Methods.

3.1. Synthetic data analysis.

To understand the information content of our algorithm as well as to choose C and k for the S_x matrix (see App. B, Eq. B5) we first do a controlled experiment using a set of "truth" data. This dataset is used to compute what the instrument would measure using the forward model (see the error discussion in Section 4). The profiles retrieved using these "synthetic" measurements are then compared with the truth to estimate the information content, and to do controlled error studies, which we will discuss in Section 4.

To construct the "truth" data we created a time-series of synthetic ozone profiles combining ozonesonde data (0-25 km) taken at Hohenpeissenberg, Germany and SAGE II data (30-60 km), and weighted averages of both in the middle atmosphere (25-30 km). SAGE data were sampled from a 20-degree wide latitude-band (37-57° N) centered at 47° N latitude, the ozonesonde station location. The time frame for the overlap of satellite and ozonesonde measurements was not limited and allowed representative (consistent) sampling of data across a month. The final set of ~1,400 profiles represents typical level of geophysical variations in ozone profile at middle northern latitudes over the 1988-1999 time period.

To test the new algorithm, we needed a synthetic data set of Umkehr measurements. Synthetic N-value data are used rather than real data in order to illustrate the difference between the various algorithm options. We used the forward model described before (Appendix A) to calculate synthetic Umkehr measurements at 12 nominal SZAs for each synthetic ozone profile. A random noise with standard deviation of 0.35 N (S_e, see Appendix B, sub-section B.7) was added to synthetic measurements to account for the noise in the measurement. The set of ozone profiles retrieved using the modified algorithm was compared with the set of synthetic profiles

(called the "truth" further on). We use synthetic data to optimize a priori covariance matrix and normalization procedure, as described below.

3.1. 1 A priori covariance matrix (S_x).

The purpose of this approach is to have a retrieval that can provide a minimum standard deviation in the monthly mean ozone values usually used to study trends. We test the algorithm for the effect of a priori on the ozone profile retrieval using four different values (0.05, 0.1, 0.2, 0.8) for coefficient $C=Var(ln\omega)$ in Rodgers definition of covariance matrix (see Appendix B, Eq. B5). The parameter k used in Eq. B5 is set to 4, since results are largely insensitive to the choice of k. Figure 1a shows standard deviation of the difference between the "truth" and the retrieved ozone profiles. The layering scheme used in this figure is described in Table 1 (see discussion in Sec 4.1). The standard deviation (SD) of the difference between the "truth" and a priori profile, SD(AP-truth), is also given for reference. The figure shows that the SD of the difference between the retrieved (RT) and the "truth" ozone profile in absence of noise, SD(RT-truth), decreases slowly as the S_x matrix increases. To include effect of noise in the test, we add a random 0.5 N-value noise to the synthesized N-values. When the noise is added to the N-values, the effect of the S_x matrix variation on the retrieved profile changes. Figure 1b shows that now the error increases when the S_x matrix is increased. Based on this finding, we suggest that S_x (0.1) provides a good compromise between capturing the variability of the atmosphere and retrieval noise. Results of the retrieval using a climatological S_x matrix (calculated from synthetic data set) have been included for comparison. Analyzing the SD(RT-Truth) shows that the retrieval error is reduced when climatological S_x was used instead of Rodgers(0.1) matrix. This observation is particularly true in the lowest layers. However, as we discuss later, the climatological S_x are not suitable for deriving the long-term trends.

Figures 1a and b also show that there is a large reduction in error (compared to the a priori) in layers 0+1 and 2+3, but there is much less reduction in upper layers, particularly with noise, because the atmospheric variability in these layers is quite small. This result is most dramatic in layer 5, where the error of the retrieved profiles with noise is about the same as the error in the a priori, which gives 0.7 correlation between the "truth" and RT layer ozone amount. Moreover, for monthly averages one can pick up some information, if the variability of the atmosphere reduces slower than the instrument noise. The instrument noise should reduce as square root of number of points averaged, assuming the noise is not correlated from one day to the next (low auto-correlation level). The atmospheric variability tends to be auto-correlated from day to day (high ozone in one day is usually followed by high ozone the next day indicating a high level of auto-correlation). The instrument noise therefore reduces much slower than the square root of number of points averaged. Figure 2 shows the results of the monthly averaged retrievals obtained with 60-degree SZA normalization. This result indicates that the monthly averaged data have a sufficient level of independent information to assess the inter-annual ozone profile variability in all layers.

3.1. 2. Normalization SZA (θ_0).

Fig. 3a shows the change in the retrieval error by changing the normalization SZA. The impact is largely in layer 0+1. The result suggests that one can change the normalization point to 70 degree SZA without adversely affecting the retrievals. One can even change the normalization to 77-degree SZA when less quality is desired from the individual profile retrieval. The only significant impact is a modest increase in noise in some

layers. For the monthly mean averaged time-series (see Fig. 3b), the errors of the retrieval using 70-degree normalization appear to be comparable to the errors of the 60-degree normalized retrieval (with the exception of layers 0+1 and 8). The retrieval without noise gets marginally worse when changing from 60 to 77 degree normalization, but with noise, the retrieval gets noticeably worse in layer 8. Nevertheless, what is so remarkable is not that the noise increases somewhat in one layer, but that the overall impact is so little. Moreover, we are dropping 4 out of 11 measurements (12, if we include total ozone) from the retrieval, and reducing the change in SZA from 30 degrees to 13 degrees, which cuts down the observation time by 60-70%. The UMK 92 algorithm varies normalization SZA with season at middle and high latitudes depending on available noontime sun elevation. Because the UMK03 algorithm's change to 70-degree SZA normalization removes the seasonal dependence in normalized N-values the small increase of errors should be an acceptable penalty to pay in this case.

3.2. Averaging Kernel.

The concept of Averaging Kernels (AK) was introduced by Rodgers [1976,1990]. The AK approach provides information on how the observed change in the atmospheric profile is distributed in the measurement system. For example, the algorithm-retrieved information can be defined as the following:

$$x_{RT} = AK \times x_T + (I - AK) \times x_{ap} + D_n \times \varepsilon \ , \qquad (2a)$$

$$AK = D_n \times K_n$$

where $\boldsymbol{x_{RT}}$, $\boldsymbol{x_{AP}}$, $\boldsymbol{x_T}$ are retrieved, a priori, and true ozone respectively, *AK* is the averaging kernel (the product of D_n and K_n matrices, which are defined in Appendix B, Eq. B3), and ε denotes measurement and forward model errors. In the absence of measurement and modeling errors, the averaging kernel tells us what the algorithm is capable of retrieving given a truth profile. The *AK* acts like a "low-pass filter", smoothing highly resolved structure of the true ozone profile. The *(I-AK)* matrix acts as a "high-pass filter" that allows highly resolved structure to propagate in the retrieved profile. Moreover, the "high-pass filter" term permits propagation of any time-dependence in a priori information to the retrieved profile as long as it has high frequency vertical structure. To demonstrate this effect we re-write Eq. 2a in the following form:

$$\hat{M} = AK \times M_T + (I - AK) \times M_{ap} + D_n \times (\bar{\varepsilon} - \varepsilon_0) \, , \qquad (2b)$$

where, $M = \dfrac{\bar{x} - \bar{x}_0}{\bar{x}_0}$, is the mean monthly ozone anomaly, subscript $\boldsymbol{T}$ denotes the true layer ozone anomaly, and $\boldsymbol{AP}$ denotes the anomaly in the layer ozone a priori, $\boldsymbol{x_0}$ denotes the mean reference layer ozone, and $\boldsymbol{(\varepsilon - \varepsilon_0)}$ represents the anomaly in stability of the instrument. The first term on the right side of the Eq. 2b shows that the AK function acts as low-pass filter to smooth out high vertical resolution features from the true anomaly. (The width of the AK can be reduced by increasing a priori covariance, but only up to a point after which the contribution matrix $\boldsymbol{D}$ increases rapidly. See the following discussion and additional information in Appendix C). The third term represents the effect of the monthly mean instrument drift on the retrieved profile, which emphasizes the importance of the instrument stability with respect to the retrieved data trend interpretation.

However, to answer the question of how the change in a priori affects the retrieved data we should examine the second term. The second term (high-pass filter) introduces high-resolution features from a priori into the retrieved profile. If a priori changes from year-to-year this change would be embedded in the retrieved data.

For example, in the Umk92 algorithm the total ozone dependent a priori information introduces a high frequency structure that varies with time. However, such a result does not honestly represent information contained in the measurements, and has a particularly serious impact on derived trends when a priori information about future trends is not available. Therefore, to minimize the effect of a priori on the retrieval, the a priori profile has to be smooth. The main benefit of a priori information to the retrieval is to reduce the bias in the retrieved data. The new UMKV8 algorithm uses an updated a priori that reduces bias in ozone profile retrieved data. Moreover, the a priori in UMKV8 algorithm does not vary from year to year, thus assuring the trend-quality of the data. Therefore, any long-term variability in the UMKV8 retrieved data is truly independent from the a priori information.

3.3 Assessment of the retrieval using AK approach.

The following examples demonstrate the AK method (additional information can be found in Appendix C and Figure C). We compare the retrieved (RT) and AK-smoothed (AK) profiles against test (OBS) profile in 61-layers. The test profile was chosen from synthetic data.

Figure 4a shows an example of a "successful" retrieval. The ozone maximum and vertical distribution are essentially captured by the retrieval. The selected profile is very smooth and does not exhibit any highly resolved features. The AK smoothed profile (which represents the retrieval under idealized measurement conditions) matches the RT profile. Their agreement provides internal validation for the retrieved profile, while the residual differences are accounted for in MSC adjustments in the retrieval process. The AP profile is very different from the observed and retrieved profiles. This example shows that under fair measurement conditions (with no measurement errors and no aerosol interference), and in case of very smooth ozone profile, the algorithm is quite capable of retrieving information from an Umkehr type measurement. However, AK-based vertical resolution analysis suggests that Umkehr retrieved ozone be assessed in 8 independent layers (Table 1).

Fig.4b shows the example of less successful high-resolution retrieval (in 61-layers). The test profile exhibits small-scale features in the troposphere, which are not picked up by the retrieval. The AK-smoothed and AP profiles suggest that although the retrieval algorithm is not able to resolve the double maxima feature in the upper troposphere, it produces a smooth solution that is different from the a priori.

3.4. Informational content of the retrieval using AK.

To better understand the informational content in the lower layers, we look at the averaging kernels in broader layers (Fig.4a). Table 1 gives a definition for these layers. The resolution of layers has been chosen to be slightly greater than the resolution of the algorithm perceived in the 61-layer AKs. Based on the 61-layer AK analysis, utilizing 60-degree SZA normalization case (. C), it seems that the simplest approach would be to combine layers 0+1+2+3. However, there are good geophysical reasons for reporting 2+3 in middle latitudes, for this combined layer represents the lower stratosphere and is strongly influenced by planetary wave activity. In addition, this layering scheme is far more convenient for data analysis than the more conservative 4-layer scheme. The lowest layer (0+1) is entirely in the troposphere, the layer above it (2+3) represents the dynamically

controlled lower stratosphere (in mid latitudes), layers 4 and 5 are defined as the transition region from dynamics to photo-chemistry, and layers 6, 7, 8, and 8+ are described as the chemically controlled region of the stratosphere.

The 8-layer scheme shows how the algorithm responds to perturbations in 8 broader layers. The numbers on the y-axis correspond to the standard Umkehr layer. Figure 5a shows that roughly half of the information in the layers shown comes from changes in the layer itself; the remaining information represents changes in the adjacent layers. It also shows that the information content in layer 0+1 and layers 2+3 is similar to the other layers. This result is contrary to what has been previously believed (Mateer et al.), where it has been claimed that lower layers contain no useful information. The information content of the lower layers was not previously realized because previous algorithms used total ozone as the a priori. Any information contained in total ozone was thus considered a part of a priori, rather than a part of the measuring system (which provides both N-values and total ozone). The total ozone measurement (in addition to the normalized N-values) is important for retrieving the ozone profile in all layers, even the uppermost layers, because every photon seen by the ground-based instrument has to pass through the total ozone column. Indeed, it can be easily shown that the largest contributor to the variance of Umkehr N-values, at even 90° SZA, is total ozone and not the variance of upper-level ozone.

The new algorithm improves ozone information in layer 8 and 8+ (see Figure 5a). The response of the 7 lower layers is about the same, but response in the top combined layer 8+ is somewhat better. The reason we suggest reporting ozone integrated above layer 8 (layer 8+), as well as ozone in individual layer 8, is that the C-pair Umkehr technique can provide layer 8+ ozone information more accurately (with less dependence on a priori) than in any other layer, including layer 8. The ozone retrieval error in layer 9+ is negatively correlated with the error in layer 8, so the combined ozone in layer 8+ is well defined. Hence, the combined ozone in layer 8+ is useful for comparing with instruments such as SBUV (Solar Backscatter Ultraviolet), which also measures combined ozone in layer 8+ more accurately than in the individual layers. When trying to split the top layer into 8 and 9+, we found that the response of layer 9+ is quite poor compared to all the other layers. Hence we do not recommend splitting layer 8+. At the same time, the response of the separate layer 8 is as good as other layers. Moreover, providing information in the combined layer 8+ only makes it difficult to compare Umkehr retrieved ozone profile with instruments like SAGE and HALOE that do not measure column amounts, and with model results. The effect of a priori on the AKs was studied. Four different values of coefficients (0.05, 0.1, 0.2, 0.8) were used in the Rodgers type covariance matrix. The corresponding AKs were inter-compared and tested to assess the level of the retrieval noise. Normally distributed random data (0.25 N-value variance) were constructed to represent measurement noise. Based on the results of synthetic data analysis, we can suggest that $\boldsymbol{Sx}$ (0.1) (see Fig. 4) provides a good compromise between capturing the variability of the atmosphere and retrieval noise for Se (0.25) that represents typical measurement noise of CMDL/NOAA automated Dobson instruments.

The effect of the measurement noise on the AKs was addressed. Fig. 4b compares AKs constructed using $\boldsymbol{Se}$ matrix with 0.25 and 2.0 N-value variance, while $\boldsymbol{Sx}$ (0.1) is the same in both cases. The results suggest that increase in $\boldsymbol{Se}$ variance from 0.25 to 2.00 N-values reduces the vertical resolution of the retrieved profile information from 2 to 2.5 layers (reduction in maximum of the fractional change from 0.5 to 0.4). Moreover, the

increase of the ***Sx***/***Se*** ratio allows model to interpret a larger part of the measurement noise into profile information, thus increasing retrieval noise. Therefore, the ***Sx*** matrix can be adjusted to improve the vertical resolution of the retrieved profile and optimize retrieval noise. Four different values of coefficients (0.1, 0.2, 0.4, 0.8) were used in the Rodgers type covariance matrix and tested to assess the level of the retrieval noise. Normally distributed random data (2.0 N-value variance) were constructed to represent measurement noise. Based on the results of synthetic data analysis, we can suggest that ***Sx*** (0.4) optimizes solution for ***Se*** (2.0). The effect of the changes in ***Se*** and ***Sx*** matrices on the retrieval noise is further discussed in Section 7.2.1.

The "best-prediction" AK calculated using a climatological Sx matrix was included for comparisons (see Fig. 5c). However, the AKs for the climatological matrix were distorted. Hence we recommend that the climatological matrices not to be used in the retrievals when ozone profile time-series to be assessed for trends.

4. Error Analysis.

All remote sensing problems, including the Umkehr technique, are susceptible to three types of errors: forward model errors, inverse model errors, and measurement errors. The radiative transfer code that we use in our forward models is in itself considered quite accurate. Errors arise primarily because one has limited information (about aerosols, for example) to model the true atmosphere or because one must make simplifying assumptions such as using fixed atmospheric temperature profiles. However, the inverse model treats errors in the measurements and forward models similarly (in Rodgers' equations, measurements $\boldsymbol{Y_m}$ and $\boldsymbol{Y_I}$ have symmetrical roles), so there is little value in improving the quality of measurements beyond what the forward model can achieve, or the inverse model can take advantage.

4.1. Forward Model Errors.

The effect of forward model error can be presented as a change in measurement, where delta-N is function of SZA. Therefore, the Rodgers contribution matrix (see Appendix B, Eq. B3) can be used to calculate the error in layer ozone:

$$\Delta\omega_n = D_n \times \Delta y \,, \qquad (3)$$

where y is normalized measurement vector and is associated with errors in the forward model when dealing with aerosols, temperature variations, MSC, surface reflectivity and total ozone. See Table 2 for the D_n coefficients (in an 8-layer scheme) calculated based on a 325 DU standard ozone profile at middle latitudes.

There are several types of errors associated with assumptions in the forward model to simplify calculations of N-values. One error is associated with the accuracy of the radiative-transfer code to produce correction tables. Petropavlovskikh et al. [2000] compared selected radiative-transfer codes to validate the accuracy of the forward model. The series of zenith-sky intensities were calculated at the ground level, at various solar zenith angles, and for a Rayleigh scattering and ozone-absorbing atmosphere, with and without stratospheric aerosols. Results of the comparisons showed that codes applying depolarization corrections to the Rayleigh scattering agreed within ±1%. The difference between zenith-sky intensities that were simulated using the vector code (polarization included) and the scalar code (no polarization included) varied overall within a 15 % range depending on solar zenith angle (SZA) and wavelength. Although, the effect of depolarization is greatly

reduced (to less than 0.8 N-values at large SZAs) by taking the ratio of zenith sky intensities (ZSIs) at two wavelengths to calculate the N-values, we still correct for the depolarization effect in multiple-scattering calculations. Petropavlovskikh et al. [2000] also compared ZSIs calculated using spherical or plane-parallel treatment of the second and higher orders of scattering. The difference in the treatment produced negligible effects on the N-values at the C-pair Dobson wavelengths. Thus, the results suggested that a vector radiative transfer code is required for the Umkehr-type studies, although full spherical treatment of zenith-sky radiation is not essential. We use the state-of-the-art vector pseudo-spherical Dave-Mateer code [Dave, 1964; Dave, 1972] for the forward model calculations.

Another error is associated with using effective absorption and scattering coefficients instead of line-by-line spectroscopic data. Applying effective coefficients in radiative transfer calculations tends to underestimate the C-pair N-values, especially at long optical paths (large SZA). The error was estimated to be within 1.5 N-value at 90-degrees SZA (after normalization to 60-degrees SZA was applied). The error depends on total ozone and on the profile. The line-by-line calculation is applied to eliminate this type of error.

4.1.1. Aerosols.

The effect of tropospheric and stratospheric aerosols on Umkehr C-pair measurements was simulated using radiative transfer code by Dave [1972 a,b]. The stratospheric aerosols are non-absorbing sulfate particles with a total optical depth of 0.1 and a vertical distribution described by Gaussian shape profiles having maximum aerosol loads at 10, 15, 20, and 25 km. The tropospheric aerosols are distinguished as either non-absorbing (sulfate particles) or absorbing aerosols with 1.0 and 0.9 single-scattering albedo, respectively. The vertical distributions for both types of tropospheric aerosols exhibit an exponential decrease with altitude when aerosol total optical thickness is fixed to 0.1. We used three different size distributions for tropospheric absorbing aerosols. However, the C-pair N-values were largely insensitive to the tested variability in size-distribution. Overall, the C-pair N-values are affected by tropospheric and stratospheric aerosols, where a 1 N-value change is equal to a –2.3 % change in radiance ratio.

Both non-absorbing and absorbing tropospheric aerosols (see example for TROP, ABS and TROP, NABS cases in Table 3a) produce a small, though non-negligible effect on the Umkehr curve, while stratospheric aerosols (see example for STR, 10, 15, 20, or 25-km cases in Table 3a) have a very large effect. N-values normalized to 60-degree SZA are not seriously affected by tropospheric aerosols, especially if aerosols are non-absorbing. As result, tropospheric aerosols do not significantly affect the retrieved ozone profile. Moreover, it appears that applying 70- or even 77-degrees SZA normalization largely reduces the non-absorbing tropospheric aerosol effect. Still, tropospheric aerosols can produce a small effect on the retrieved ozone profile, especially at the upper stratosphere and lower troposphere. Our analyses indicate that interference from tropospheric aerosols can result in a 3.5 % deficit of the retrieved ozone in layer 8, and a 6 % excess for retrieved ozone in layer 0+1 (our analysis is done for 0.3 optical depth, which is typical annual averaged value for local pollution, see Table 3b for more details). Moreover, if absorbing aerosols are located at higher altitudes (up to 10 km), the effect becomes more serious, and the deficiency in the retrieved ozone in layer 8 can be as large as 10 percent.

At the same time, the effect of stratospheric aerosols on retrieved ozone can be significant [i.e. Mateer and DeLuisi, 1992]. Stratospheric aerosols affect ozone profile products and produce significant errors (although

at much shorter periods of time than local pollution). The error due to aerosol effect on N-values (see Table 3a for examples) can be calculated using Eq. 3 (see Table 3b for corresponding examples). Note that values from Table 3a can be used only after the normalization is applied. For example, the user should subtract the N-value at 60-degrees SZA (first column) from all N-values in the selected row in Table 3a. (Note, full vector radiative-transfer code should be used when calculating aerosol error effects. Petropavlovskikh et al. [2000] showed that scalar radiative-transfer codes overestimate aerosol errors by about 20 %.)

4.1.2. Multiple scattering.

The multiple scattering (MSC) error is associated with the use of tables to account for the second and higher orders of scattering. The consistency between N_{MSC} tables and the first guess ozone profile is warranted by the fact that the same set of the climatological ozone profiles is used to create tables. We propose to use individual MSC tables for each station to account for altitude dependence in MSC. The seasonal change of ground albedo also affects the MSC, however the effect is not SZA dependent and is reduced by normalization. The algorithm uses pre-calculated MSC, which are a piecewise linear fit to the total ozone. However, the error in the observed total ozone can produce an error in the MSC estimates. Table 4 lists the change in N-values due to errors in total ozone. The problem of fast changes in total ozone during the measurement time is not addressed in this paper.

A new feature in the updated algorithm allows adjusting the tabulated MSC at each step of iteration to reflect the difference between observed and standard ozone profiles. The MSC Jacobian matrix is pre-tabulated for a set of standard first guess profiles, and it is linearly interpolated to match observed total ozone. The MSC Jacobian matrix (see Appendix A, Eq. B1) is applied to a difference between the retrieved and the standard first guess ozone profiles to calculate an adjustment to MSC tabulated N-values. Errors of less than 0.05 N-values are possible because the Jacobian matrix depends on both the profile and total ozone.

4.1.3. Surface reflectivity.

We have looked at the effect of the ground reflectivity variations on ZSI measurements. We found that there is an about 4 N-value increase in the Umkehr measurement for the Dobson C-pair for 60-percent change in surface reflectivity (relative to zero-reflectivity calculations). However, the increase in the Umkehr measurement has virtually no SZA dependence. It is clear that surface reflectivity has no effect on normalized N-values and thus will not affect Umkehr ozone profile retrievals [Dütsch and Staehelin, 1992]. This result suggests another reason for normalizing the Umkehr curve. Clouds that are not in the instrument's field of view may have a similar effect as surface reflectivity, but this assertion requires field-testing.

4.2. Inverse model errors.

Other errors can be introduced by the inverse models, and include effects from the a priori information, from measurement noise, or from the temperature dependence of ozone cross sections.

4.2.1. A priori and measurement noise.

Table 5 lists the standard deviations for retrieval errors in 8 layers, associated with the use of a priori information (***Sx***=0.1), the noise of normalized Umkehr measurement (***Se***=0.25), and total ozone measurements (the standard error of 3 DU). The retrieval is done with 70-degree SZA normalization. The first row shows retrieval errors due to a priori information. The second row shows retrieval errors due to both sources of errors. Errors in the total ozone can affect estimates of the $\boldsymbol{N_{ms}}$ (Table 4), and can also influence the retrieval. This effect occurs because the total ozone measurement is used as conservation factor in place of the measurement used in the normalization procedures. The effect of the increased measurement noise (***Se***=2.0) on the retrieval noise (due to both sources of errors) is summarized in the third row of the Table 5. Errors of the retrieval associated with increases in both measurement (Se=2.0) and a priori information (Sx=0.4) variance are shown in the 4th row of the table. The 5th and the 6th rows summarize effect of the measurement noise on monthly averaged retrievals in 8 layers.

The impact of the measurement noise on the accuracy of the retrieved ozone profile can be evaluated from covariance of the retrieval noise (Rodgers, 2002, Eq. 2.19):

$$S_m = D_n S_e D_n^T,$$

where ***Dn*** (Appendix B, Eq. B4) is the contribution matrix, and ***Se*** is the measurement noise matrix, where noise is considered to be random, unbiased and uncorrelated. Table 6 summarizes errors in the retrieved ozone profile caused by three types of noise: low-level noise (0.5 N-value), high-level noise (1.4 N-value), and SZA dependent noise (see Appendix B.7 and Table B for details). Results show an increase in the retrieval noise with higher level of the measurement noise. However, when measurement errors increase with SZA, the primary impact on the retrieval errors is found in the upper layers. These results agree with the fact that measurements at large SZAs are especially sensitive to ozone variability in the upper stratospheric layers. Therefore, elevated errors at the large SZAs would strongly contribute to the accuracy of the retrieved ozone in upper atmospheric layers.

4.2.2 Atmospheric Temperature.

The ozone absorption cross sections that are used in the forward model are temperature dependent. The temperature profile used in our retrievals is a single middle-latitude average profile. According to Mateer and DeLuisi [1992], the errors in the retrieved ozone profile can be within ± 4 %, depending on the seasonal or latitude difference between observed and averaged temperature profiles. We use a temperature profile climatology that is monthly and zonal-averaged (10-degree band; Summer et al., 1993) to correct for seasonal temperature dependence in the observed N-values.

From Komhyr et al. [1993], the temperature dependence of Dobson C-pair is 0.14%/degree C change in atmospheric temperature. Therefore, we estimate that a 7-degree error in the temperature in a layer (using the 8-layer scheme) will produce a 0.5 to 1% error in ozone depending on the vertical distribution of the temperature. The smaller value applies if the temperature error is confined to a single layer, while the larger value applies if the temperature error varies slowly with height.

5. Retrieval of a test trend model

A test of the Umkehr retrieval algorithm's ability to capture predicted trends in the ozone profile has been performed. Each Umkehr layer is divided into 4 sub-layers. The estimated trend in the ozone profile [Miller et al., 1996] as derived from SAGE II and ozone-sonde measurements in the northern middle latitudes has been used to study the performance of the new algorithm. Fig. 6a shows vertical distribution of ozone changes (in DU) represented in 61-layers (marked as RT in the plot). The trend predicted using the method of Averaging Kernels (AK) is also shown. This test demonstrates the best that the Dobson can do to detect ozone profile changes. For small changes in the ozone profile, the AK method provides a very quick and very accurate way of assessing the algorithm's response.

Results of the comparisons show fairly good agreement between the retrieved (RT) and predicted (AK) trends, even at high vertical resolution. The Umkehr algorithm predicts a secondary minimum in the ozone trend in the lower stratosphere, although it places the maximum at a higher altitude than expected. Fig. 6a indicates that the Umkehr method underestimates the ozone trend below 20 km. However, an apparent difference between the large positive trend below 10 km seen by ozonesondes and the small positive trend seen by Umkehr results from plotting results at a higher resolution, thus misrepresenting the ozone profile information contained in the Umkehr retrieval. The Umkehr ozone profile information has only limited resolution (about 10 km) in the troposphere, as can be deduced by examining the AKs (Appendix C). All comparisons in the troposphere (0-20 km) should be done after combining the high-resolution ozone profile into two 10-km-wide layers. This test trend represents an extreme case of the large and steep increase of tropospheric ozone. However, after combining the profile into 8 layers as described above, Fig. 6b shows that the expected trend in the lowermost 10-km layer is only +2.5 % whereas the RT results give +1% change. Results of the UMK92 retrieval (TOAP) are also given for comparison.

6. Conclusion.

The new UMKv8 algorithm is designed to capture the ozone trend without algorithm interference. The need to develop a new retrieval algorithm comes from the fact that a priori profiles used in the TOAP (UMK92) algorithm are constructed using total ozone measured by Dobson in the direct sun mode. Although there is nothing inherently wrong with this approach, it makes the error analysis of the retrieved profile difficult by introducing short- and long-term variability other than the customary seasonal and latitudinal changes. The variability makes it difficult to ascertain if the observed long-term changes were forced by a priori or are a part of the measurements. Mateer and DeLuisi [1992] chose not to use the traditional method of basing the a priori climatology on season and latitude only, for they felt that the profile variations due to total ozone were too large and better results would be obtained if the a priori were normalized to contain the same total ozone as the measured total ozone.

We made several changes to the algorithm. First, in our new updated algorithm UMK03 we use the more traditional approach of basing our a priori climatology on season and latitude only. Thus, the new a priori profile has no short-term, inter-annual, or long-term variability. The inter-annual variability in the retrieved

ozone can then be easily separated from the a priori information. Second, we reformulate the retrieval problem to make it nearly linear, thus requiring less a priori information to obtain stable solutions. Third, we increase the vertical resolution of the solution. This approach minimizes the errors of the retrieval caused by interpolation procedures, where the lower-resolved inverse model solution has to be repeatedly converted to the highly resolved profile utilized in the forward model. Fourth, we allow for a solar zenith dependence in the measurement noise in the retrieval. Fifth, in order to achieve trend–quality data and minimize effect of a priori on the retrieved data we change the a priori covariance matrix based on Rodgers recommendations.

Our results indicate it is possible to construct an algorithm that can handle large variations in total ozone with no adverse effects. Our overall results are virtually the same as the Mateer and DeLuisi algorithm, but the improved algorithm has no a priori dependence, and it is more linear, which simplifies analysis of retrieval errors. Further information on the a priori ozone profiles for 12 months and AK, as well as a table for a full resolution 61-layer AK is available at http://www.srrb.noaa.gov/research/umkehr. Readers can use the provided information to predict how the Umkehr retrieval would respond to alternative trend scenarios. The advantage of the method is that the AK can be applied directly to ozone mixing ratio profiles without first converting them to Dobson units. We have made several other improvements, though they would be less noticeable to the end user. We have tested our algorithm extensively by constructing a synthetic data set.

Our three key findings are as follows:

First, we recommend that the Umkehr profiles should be reported and analyzed in 8 layers obtained by combining the 10 original layers as follows (0+1, 2+3, 4, 5, 6, 7, 8, 8+.). Note that traditional layer 1 has always been a double layer and is essentially the same layer as 0+1 layer discussed in this paper. We are recommending that layer 2 and 3 be similarly combined, as there is no information in the measurements to separate them. We also recommend that layer 8 should be combined with all the layers above it to form a single layer. Our extensive analysis using synthetic data indicates that the recommended 8 layers contain reasonably independent information, meaning that the retrieval errors are not significantly correlated. However, it is important to remember that the AK analysis indicates that the retrieval resolution from Umkehr is somewhat worse than the width of these 8 layers. Thus, one cannot expect perfect retrievals even in the reduced 8-layer system.

Second, our error analysis indicates that if the total column ozone is known reasonably accurately, and the instrument is properly calibrated, there is useful information in the tropospheric layer (253-1013 hPa), of roughly the same quality as in the other 7 layers. However, the comparisons with the real Umkehr data and the sondes are too noisy to make a definite conclusion.

Third, we recommend changing the normalization to 70-degree SZA regardless availability of the measurements at lower SZAs. Unless we can provide a compelling case that layer 1 ozone can be reliably obtained from Umkehr, we could even recommend changing the normalization of Umkehr N-values to a SZA of up to 74 degrees. Although we do lose information in layer 1, we can reduce the measurement time by one half to two thirds, reducing the chances of atmospheric variability, and perhaps better canceling out the wedge calibration error.

The question of "How much information do we lose when we change normalization from 60 to 77 degree SZA?" has contradictory answers, ranging from very little to somewhat significant. The consequence of going to 77-degree SZA normalization would be an increase in the RT error. Because this approach might reduce systematic errors due to a wedge calibration, the increased noise in the layer-8 retrieved ozone may be an acceptable penalty to pay in particular cases. We suggest that in high latitudes, when the noontime SZA reaches 70 degrees or more, using a 77-degree normalization at high latitudes will reduce observing time while enabling good quality retrievals. We therefore recommend that the high latitude stations, particularly the automated Dobson and Brewer stations, should collect Umkehr data even when the noontime SZA is relatively low. Still, the key question about reducing (or increasing) systematic errors by changing the normalization from 60 to 70 or even to 77-degrees SZA cannot be answered using the synthetic dataset. We will examine this issue using real data in a future paper.

This study has also revealed an important application of the N-value residuals. Analysis of these residuals can detect subtle deficiencies of the inverse model better than AK or the standard deviations of the retrieved minus true ozone. Future studies of the N-value residuals should be conducted using real data. We expect to see the instrumental errors more clearly than with any other technique, particularly those techniques that are purely statistical. Another use of the N-value residuals would be to search for a stratospheric aerosol signature. It is possible to develop an analytical method to flag, and perhaps even correct, the data.

A future paper will look at how these results reported here can be applied to automated Dobson and Brewer Umkehr data. We will address the main question of how much information can be gained by reducing noise in the measurements. We will also examine the advantage of using multiple wavelength pairs.

References

Bass, A.M., and R.J. Paur, The ultraviolet cross-section of ozone: I. The measurements, in Atmospheric Ozone, *Proc. Quadrennial Ozone Symposium*, edited by C.S. Zerefos and A. Ghazi, pp.601-606, Reidel publ., 1985.

Bhartia, P. K., D. Silberstein, B. Monosmith, and A. J. Fleig, Standard profiles of ozone from ground to 60 km obtained by combining satellite and ground base measurements, in *Atmospheric Ozone,* edited by C. S. Zerefos and A. Chazi, pp. 243-247, D. Reidel, Dordrecht., 1985.

Bhartia, P. K., R. D. McPeters, C.L. Mateer, L. E. Flynn, and C. Wellemeyer, Algorithm for the estimation of vertical ozone profiles from the backscattered ultraviolet technique, *J. Geophys. Res*., 101, 18,793-18,806, 1996.

Chapman, S., A theory of upper atmospheric ozone, Mem. Roy. Met. Soc., 3, 103, 1930.

Cunnold, D.M., M.J. Newchurch, L.E. Flynn, H.J. Wang, J.M. Russell, R. McPeters, J.M. Zawodny, and L. Froidevaux, Uncertainties in upper stratospheric ozone trends from 1979 to 1996, J. Geophys. Res., 105, 4427-4444, 2000

Dave, J. V., Multiple scattering in a non-homogeneous atmosphere, J. Atmos. Sci., 22, 273, 1964.

Dave, J. V., Development of programs for computing characteristics of ultraviolet radiation, Technical report- Scalar Case, IBM Corp., Fed. Syst. Div., Gaithersburg, Md., 1972a

Dave, J. V., Development of programs for computing characteristics of ultraviolet radiation, Technical report - Vector Case, IBM Corp., Fed. Syst. Div., Gaithersburg, Md., 1972b

DeLuisi, J. J., and C. L. Mateer, On the application of the optimum statistical inversion technique to the evaluation of the Umkehr observations, *J. Appl. Meteor.*., 10, 328-334, 1971.

DeLuisi, J. J., D. U. Longenecker, C. L. Mateer, and D. J. Wuebbles, An analysis of northern middle-latitude Umkehr measurements corrected for stratospheric aerosols for 1979-1986, *J. Geophys. Res*., 94, 9837-9846, 1994.

DeLuisi, J. J., D. U. Longenecker, P. K. Bhartia, S. Taylor, and C. L. Mateer, Ozone profiles by Umkehr, SBUV, and Ozonesonde: A Comparison including the inversion algorithms for Umkehr and SBUV, in *Ozone in the Atmosphere*, edited by R. D. Bojkov and P. Fabian, pp. 206-210, A Deepak, Hampton, Va., 1989.

Dobson, G. M. B., Observations of the amount of ozone in the Earth's atmosphere and its relation to other geophysical conditions. Part IV, Proc. Roy. Soc., London, A129, 411-433, 1930.

Dobson, G.M.B., Observers' handbook for the ozone spectrophotometer, Ann. I. G. Y., 5 (1), 46-89, 1957.

Dütsch, H.U., Evaluation of the Umkehr effect by means of a digital electronic computer. *Sci. Rep. No. 1*, Ozone and general circulation in the atmosphere, Arosa, Lichtklimatiches Observatorium, 1957.

Dütsch, H. U., Vertical ozone distribution from Umkehr observations, *Arch. Met. Geophys. Biokl.*, *A11*, 240-251, 1959.

Dütsch, H. U. and J. Staehelin, Results of the new and old Umkehr algorithm compared with ozone soundings, J. Atmos. and Terr. Phys., 54, pp.557-569, 1992

Elansky, N. F, I. V. Mitin, O. V. Postylyakov, Maximum accuracy of Umkehr measurements of vertical ozone profiles, Izvestiya,,

Flittner, D. E.; Bhartia, P. K.; Herman, B. M., O3 profiles retrieved from limb scatter measurements: Theory, *Geophys. Res. Lett*., **27**, no. 17 , p. 2601-2604 (1999GL011343), 2000.

Atmospheric and Oceanic Physics, Washington, DC, vol. 35, no. 1, pp. 65-77, 1999.

Götz, F.W.P., Zum Stralungsklima des Spitzbergen Sommers: Stralungs und Ozonmessungen in der Königsbucht 1929, *Gerlands Beitrage zur Geophys., 31,* 119-154, 1931.

Götz, F.W.P., A.R. Meetham and G.M.B. Dobson, The vertical distribution of ozone in the atmosphere, Proc. Roy. Soc. London a145, 416-443, 1934

Harris, N., R. Hudson, and C. Phillips, SPARC/IOC/GAW Assessment of Trends in the Vertical Distribution of Ozone, pp. 289, World Climate Research Program of WMO/ICSU, 1998.

Komhyr, W. D., Operations Handbook – Ozone Observations with a Dobson Spectrophotometer, WMO Global Ozone Research Project, Report No. 6, Geneva, 1980.

Komhyr, W.D., R.D. Grass and R.K. Leonard, Dobson Spectrophotometer 83: A Standard for Total Ozone Measurements, 1962-1987, J. Geophys. Res., D7, 94:9847-9861, July 20, 1989

Komhyr, W.D., C.L. Mateer, R.H. Hudson, Effective Bass-Paur 1985 Ozone absorption coefficients for use with Dobson ozone spectrophotometers, J. Geophys. Res., D11, 20,451-20.465, 1993.

Mateer, C.L., A study of the information content of Umkehr Observations. Ph. D. thesis, University of Michigan, 1964.

Mateer, C.L., and H.U. Dütsch, Uniform evaluation of Umkehr observations from the world ozone network, pp. 105, National Center for Atmospheric Research, Boulder, CO, 1964.

Mateer, C. L., A review of some aspects of inferring the ozone profile by inversion of ultraviolet radiance measurements, in *Mathematics of Profile Inversion*, edited by L. Colin, NASA Ames Res. Cent., Moffet Field, Calif., 1971.

Mateer, C. L., D. F. Heath, and A. J. Krueger, Estimation of total ozone from satellite measurement5s of back-scattered ultraviolet Earth radiance, J. Atmos. Sci., 28, 11307-1311, 1971.

Mateer, C. L. and J. J. DeLuisi, A new Umkehr inversion algorithm, *J. Atmos. Ter. Phys., 54,* 537–556, 1992.

Mateer, C.L., H.U. Dutsch, J. Staehelin, and J. J. DeLuisi, Influence of a priori profiles on trend calculations from Umkehr data, *J. Geophys. Res*., **101**, 16779-16787, 1996.

McElroy, C.T. and J.B. Kerr, Table mountain ozone intercomparison: Brewer ozone spectrophotometer Umkehr observations, J. Geophys. Res., 100, 9293-9300, 1995

McPeters, R.D., et al., Earth Probe Total Ozone Mapping Spectrometer (TOMS) Data Products User's Guide, *NASA/TP-1998-206895*, 1993

McPeters, and B. J. Connor, Comparison of NOAA-11 SBUV/2 ozone vertical profiles with correlative measurements, Geophys. Res. Lett., 23, pp. 293-296, 1996

Miller, A.J., L.E. Flynn, S.M. Hollandsworth, J.J. DeLuisi, I.V. Petropavlovskikh, G.C. Tiao, G.C. Reinsel, D. J. Wuebbles, J. Kerr, R.M. Nagatani, L. Bishop, and C.H. Jackman, Information content of Umkehr and solar back-scattered ultraviolet (SBUV) 2 satellite data for ozone trends and solar responses in the stratosphere, J. Geophys. Res., **102**, 19,257-19,263, 1997.

Newchurch, M. J., D. M. Cunnold, and J. Cao, Intercomparisons of Stratospheric Aerosol and Gas Experiment (SAGE) with Umkehr[64] and Umkehr[92] ozone profiles and time series: 1979-1991, J. Geophys. Res., **103**, 31,277-31,292, 1998.

Newchurch, M.J., L. Bishop, D.M. Cunnold, L. E. Flynn, S. Godin, S.H. Frith, L. Hood, A. J. Miller, S. Oltmans, W. Randel, G. Reinsel, R. Stolarski, R. Wang, E.S. Yang, and J.M. Zawodny, Upper-stratospheric ozone trends 1979-1998, *J. Geophys. Res.*, *In Press*, 2000.

Petropavlovskikh, I. V., J. J. DeLuisi, R. Loughman, B. Herman, A Comparison of UV Intensities Calculated by Spherical-Atmosphere Radiation Transfer Codes: Implications for Improvement to the Umkehr Method, *J. Geophys. Res.*, **105**, 14,373-14,746, 2000.

Petropavlovskikh, I. V., J. DeLuisi, D. Theisen, R. Bojkov, P.K. Bhartia, Detection of Shifts in the Umkehr N-value Radiance Records, in press, *Geophys. Res. Lett*., **28**, 255-258, 2001.

Planet, W. G., A. J. Miller, J. J. DeLuisi, D. J. Hofmann, S. J. Oltmans, J. D. Wild, I. S. McDermid, R. M. McPeters, and B. J. Connors, Comparison of NOAA-11 SBUV/2 ozone vertical profiles with correlative measurements, *J. Geophys. Res.*, **23**, 293-296, 1996.

Randel, W.J., R.S. Stolarski, D.M. Cunnold, J.A. Logan, M.J. Newchurch, and J.M. Zawodny, Trends in the Vertical Distribution of Ozone, *Science*, *285*, 1689-1692, 1999

Rodgers, C. D., Retrieval of atmospheric temperature and composition from remote measurements of thermal radiation, *Re. Geophys. Space Phys.,* **14**, 609-624, 1976.

Rodgers, C. D., Characterization and error analysis of profiles retrieved from remote sounding neasurements, *J. Geophys. Res.*, **95**, 5587-5595, 1990.

Reinsel, G. C., G. C. Tiao, A. J. Miller, R.M. Nagatani, D. J. Wuebbles, E.C. Weatherhead, W.-K. Cheang, L. Zhang, L.E. Flynn, and J. Kerr, , Update of Umkehr ozone profile data trend analysis through 1997, *Geophys. Res. Lett.,* **104**, 23,881-23,898, 1999.

Strand, O. N. and E. R. Westwater, Statistical estimation of the numeric solution of a Fredholm equation of the first kind, *J. Ass. Comput. Mach.,* **15**, p. 100, 1968.

Summers, M. E., W. Sawchuck, "*Zonally Averaged Trace Constituent Climatology. A Combination of Observational Data Sets and 1-D and 2-D Chemical-Dynamical Model Result",* Naval Research Laboratory, Technical Report, NRL/MR/7641-93-7416, *Washington, DC.,* 1993.

Westwater, E. R., and O. N. Strand, Statistical information content of radiation measurements used in indirect sensing, *J. Atmos. Sci.,* **25**, p. 750, 1968.

World Meteorological Organization, *Report of the International Ozone Trend Panel, WMO Global Ozone Research and Monitoring Project, Rep.* ***18****.,* Geneva, 1988a.

World Meteorological Organization, The Fifth Biennial WMO Consultation on Brewer Ozone and UV Spectrometer Operation, Calibration and Data Reporting, McElroy, C.T. and E.W. Hare (editors), WMO Report No 139, Halkidiki, Greece, September 1998b (Published in 2000).

WMO, Scientific Assessment of Ozone Depletion - 1998, WMO Global Ozone Research Project, Report No. 44, Geneva, 1998c.

WMO, Five Years of Ozone and UV Data from the Brewer Spectrophotometer at Bedford, N.S. 1993-97, Report MAES 1-98, Keith N. Keddy, Billie L. Beattie and Cindy N. Vallis, Environment Canada, August 1998d.

WMO, Consultation on Brewer Ozone Spectrophotometer Operation, Calibration and Data Reporting. Report No. 22, Arosa, Switzerland, August 1990.

Appendix A. Detailed description of the Forward model.

A.1 Spectroscopique data set.

The input dataset is based on cross-sections, α, for ozone absorption measured by Bass and Paur [1984]: $\alpha=C_0+C_1T+C_2T^2$, where T is temperature, C_0 is ozone absorption at 0^0C, and C_1 and C_2 are linear and quadratic temperature correction coefficients respectively. The Rayleigh scattering cross-section, β, are from Bates [1984]. The forward model uses absorption and scattering coefficients ($atm^{-1}cm^{-1}$ and atm^{-1}), that are converted from cross-sections by assuming 2.149 X 10^{25} air molecules/cm^2 in 1 *atm* column of air [Pendorf, 1957] and 2.6868 x 10^{19} O_3 molecules/cm^2 in 1 *atm-cm* column of ozone. The Dobson C-pair band passes are published by [Komhyr et al., 1993].

A.2 N-value calculation

The radiative-transfer equation is an algebraic representation of the relation between ozone vertical distribution and zenith-sky measurements at different solar zenith angles.

Because it is too expensive to run a full radiative-transfer code, for efficiency we separate total radiance (N_{TOT}) into four components: a first component that includes only single-scattered radiances (N_{SS}); a second component that contains secondary and higher orders of scattered radiances (N_{MSC}); the third component that represents refraction (N_R), and the fourth component allows for temperature correction (N_T):

$$N_{TOT} = N_{SS} + N_{MSC} + N_R + N_T \qquad \text{(A1)}$$

The N_{SS} is calculated using a 61-layer (each layer is one fourth of the nominal Umkehr layer, about 1.2 km wide) vertical profile scheme inside of the program [Mateer, 1964]. The single-scattered zenith-sky intensity (I) at a given wavelength can be described as following:

$$I_\lambda = I_\lambda^0 \times \beta \times P(\theta) \int_{p0}^{\infty} \exp\left[-\int_{p0}^{p} (\alpha_\lambda dx_3 + \beta_\lambda dp) - \int_{p}^{\infty} (\alpha_\lambda dx_3 + \beta_\lambda dp) \cdot ds / \Delta h \right] \cdot dp / \Delta p \text{ , (A2)}$$

where I_λ^0 is the spectral radiance outside the earth's atmosphere, $P(\theta)$ is scattering function, θ is scattering SZA, α_λ and β_λ are ozone absorption and Rayleigh scattering coefficients (cm^{-1}) respectively (described above), dx_3 (atm-cm) is ozone amount in layer dp, ds is slant path of incidence of direct beam in layer dp (*atm*) of Δh (*km*) thickness, and p_0 is the pressure altitude of the station, Δp is change in pressure of sub-layer (*atm*). The geometric slant path is used for each layer except for the top layer (3.052E-2 hPa atm and above) where the Chapman function is used to estimate the slant path.

A.3 Line-by-line calculation.

The forward model provides line-by-line calculations of spectrally resolved zenith-sky radiances per unit solar flux. The Dobson band-passes are relatively wide (1.4 and 3.2 nm). Therefore, to simulate Umkehr measurement the highly resolved spectral radiances are convoluted with solar spectrum over the band-passes (S_λ) for C-pair wavelength [Komhyr et al, 1993]:

$$I = \frac{\sum_{\lambda} I_\lambda \times I_\lambda^0 \times S_\lambda \times \partial\lambda}{\sum_{\lambda} I_\lambda^0 \times S_\lambda \times \partial\lambda} \quad \text{(A3).}$$

We use Eq. A2 to calculate first-guess single-scattering N-values, N_{SS}, at nominal SZAs. The first order partial derivatives ($\partial N_{SS}/\partial X$), or single-scattering Jacobian matrices, are calculated analytically by differentiating the radiance, or forward model element, defined in Eq. (A3) with respect to a state vector element, or layer ozone amount X. The N_{MSC} and multiple-scattering Jacobian matrices, $\partial N_{MSC}/\partial X$, are pre-calculated and tabulated at 1 and 0.5 atm pressure-levels, using full vector Dave-Mateer code [Dave, 1964; Dave, 1972]. The tabulated N_{MSC} and Jacobians are based on the updated set of standard ozone profiles (see Section 4.5). The tabulated N_{MSC} and Jacobians are linearly interpolated to the altitude of the individual Dobson station location and to the total ozone observed at the station.

A.4 Jacobian or weighting function.

Fig.A provides an example of the Jacobian matrix, $\partial N/\partial lnX$, or so-called weighting functions, as a function of altitude and SZA. The Umkehr C-pair weighting functions are shown after applying total ozone normalization:

$$\frac{\partial N_{adj}(\theta)}{\partial \ln(X)} = \frac{\partial N_{adj}(\theta)}{\partial X} \times X = \left[\frac{\partial N(\theta)}{\partial X} - \frac{\partial N(\theta)}{\partial \Omega} \right] \times X , \quad \text{(A4)}$$

where $\partial N(\theta)/\partial \Omega$ is partial derivative that defines sensitivity of N-value at nominal SZA, θ, to total the ozone, Ω. The last term on the right in Eq. (A4) is estimated using polynomial fit of the second order to N-values as function of total ozone (total ozone is normalized to mean middle latitude value of 325 DU). We synthesize Umkehr C-pair N-values for a set of standard ozone profiles (see Section B.5) using our forward model as described above. As a result, the N-value at nominal SZA, θ, can be defined as following:

$$N(\theta) = A(\theta) + B(\theta) \times (\Omega - 325) + C(\theta) \times (\Omega - 325)^2 , \quad \text{(A5)}$$

where A, or N-value for 325 DU total ozone standard profile, B and C are coefficients of the polynomial fit and are provided in Table A as function of SZA. Therefore, based on the polynomial fit we derive partial derivative of the N-value with respect to the total ozone as following:

$$\frac{\partial N(\theta)}{\partial \Omega} = B(\theta) + 2C(\theta) \times (\Omega - 325). \quad \text{(A6)}$$

Figure A truly reveals the profile information of the Umkehr technique. Plots of the total ozone normalized weighting functions make it clear that there is virtually no profile information in N-values at 60, 65, and 70 – degrees SZAs, whereas functions at other SZAs are sensitive to ozone variations at different altitude levels.

The new UMK03 algorithm includes a provision to adjust N_{MSC} to reflect the departure in the retrieved ozone profile from the standard profile:

$$N_{MSC}^{RT} = N_{MSC}^{STD} + \frac{\partial N_{MS}}{\partial X}(X_{RT} - X_{STD}), \quad \text{(A7)}$$

where N_{MSC}^{STD} is tabulated correction, $\partial N_{MS}/\partial X$ is tabulated multiple-scattering Jacobian matrix, X_{RT} and X_{STD} is retrieved and standard ozone respectively.

A.4 Refraction and temperature corrections.

The refraction correction, N_R, tables at sea level, 1 atm, and 0.5 atm are pre-calculated using TOMRAD code, which is based on full vector Dave-Mateer code [Flitner et al., 2000]. The N_R is linearly adjusted to the altitude of the station.

The temperature correction, N_T, is done in the forward model to account for seasonal variations in the temperature profiles. We use NRL climatology of standard temperature profiles [Summers and Sawchuck, 1993] that are tabulated as function of latitude and month. The dependence of the ozone absorption cross-section, $\boldsymbol{\alpha}$, on temperature variations may create seasonal signatures in the Umkehr measurements (see Eq. A2). Therefore, we can write the change in $\boldsymbol{N}$ due to the change in absorption cross section $\boldsymbol{\alpha}$ as:

$$\Delta N = \sum_j \frac{\partial N}{\partial \alpha_j} \Delta \alpha_j , \qquad \text{j=1,….M} \qquad \text{(A8)}$$

where Σ is the integral over M wavelengths within band-pass. In addition, the change in absorption cross-section, $\Delta\alpha_j$, due to the change in temperature can be expressed as:

$$\Delta \alpha_j = C_1 \left(T - T_0\right) + C_2 \left(T^2 - T_0^2\right), \qquad \text{(A9)}$$

where $\boldsymbol{T}$ is the seasonal temperature, $\boldsymbol{T_0}$ is the nominal temperature, and C_1 *and* C_2 are linear and quadratic temperature correction coefficients for ozone absorption coefficient respectively. After assuming that change of the layer ozone is proportional to the change of absorption cross-section in the log space, we can define temperature correction, $N_T=\Delta N$, as:

$$N_T = \sum_i \frac{\partial N}{\partial x_i} \frac{x_i}{\alpha_j} \left[\alpha_j^1 \left(T - T_0\right) + \alpha_j^2 \left(T^2 - T_0^2\right)\right], \qquad \text{i=1,…,N} \qquad \text{(A10)}$$

where Σ is the integral over N atmospheric layers.

Appendix B. Details of the Inverse Model.

B.1 Inverse Model description.

Remote sensing methods present a non-linear problem when atmospheric information contained in the measurement has to be retrieved. If the problem can be simplified, it is reduced to a linear relation between measurements and the sought atmospheric parameters (the ozone profile in our case). The common methods utilize a Newtonian technique, where information is expanded in a Taylor series around the a priori vector:

$$y = y_1 + \frac{\partial y}{\partial x} * \Delta x + o(\Delta x)^2 \qquad \text{(B1)}$$

where y is the measurement vector, y_1 is the predicted measurement vector based on the first guess information, and x is the state vector, and the last term on the right represents the higher order terms in the equation that are typically very small and are added iteratively

Rodgers [1976, see Eq. 101] provides the following equation for the inverse problem:

$$x_{n+1} = x_0 + D_n \times \left[y - y_n - K_n \left(x_0 - x_n \right) \right], \qquad \text{n=1,…N} \qquad \text{(B2)}$$

$$D_n = S_x K_n^T \left(K_n S_x K_n^T + S_e \right)^{-1} \qquad \text{(B3)}$$

where x_{n+1} is the state vector for the solution of the iterative equation, and $x_n \rightarrow X$ (truth) when $n \rightarrow \infty$, x_0 is the *a priori* (guessed) information, S_x is the *a priori* covariance matrix, $S_e = K_n X$ is the measurement error matrix, $K_n = dy/dx$, is a Jacobian matrix, y is the measurement vector, y_n is the predicted measurement vector for the state vector x_n, and D_n is the Rodgers contribution function. Although Mateer and DeLuisi [1992] chose $x_1 = x_0$ to initialize the inverse model, we make distinction between x_0 and x_1, where x_0 is a priori, and x_1 is a "good" first guess used to pre-calculate the MSC and Jacobian matrix tables. All of these parameters are discussed further in this section.

B.2 State vector (x_n).

The state vector x_n in Eq. (B1) is defined as a retrieved ozone profile. In UMK03 algorithm the state vector is defined as layer ozone amount ($x_n = \omega$) in DU (1DU=10^{-3} atm-cm). In Umk92 algorithm, the state vector is defined as the log of ozone ($x = ln(\omega)$) in nominal Umkehr layer to avoid negative ozone values in solution for the individual layer. However, because N-values vary approximately linearly with layer ozone, errors in N-values, such as measurement noise, produce retrieval errors in ozone that are roughly independent of layer ozone. So, the use of $ln(\omega)$ distorts the statistics in layers where the retrieval errors are large (e.g., layers 2 and 3)). The problem is particularly serious when the layer ozone is close to zero, for example, for layer 2 in the tropics and layers 2 and 3 in the ozone hole. Using $ln(\omega)$ forces the retrieval to produce only positive layer ozone values, biasing the mean. Our algorithm allows ozone in these layers to fluctuate on both sides of zero.

We also use a 61 layer (¼ of the traditional Umkehr layer, approximately 1.2 km wide) retrieval scheme as opposed to the 12 layer Mateer scheme to avoid fitting a spline to convert from the retrieved layer ozone to the high resolution layers in the forward model. Rodgers (private communication) has remarked that use of the

lower-resolution layering introduces representational errors, which are easily avoided by using the same layering scheme for the retrievals and for the forward model calculations.

B.3 A priori (x_0).

The a priori information was developed using a new ozone climatology [ref. Labow, 2000?], which had been generated, using monthly mean of sonde measurements below 25 km, and SAGE (Stratospheric Aerosol and Gas Experiment) and MLS (Microwave Limb Sounder) data in upper stratosphere. These data are converted to Umkehr layers, averaged over 10-degree latitude bands, and then fitted as a function of day number only. This procedure is principally different from that used previously for UMK92 algorithm, where the a priori was adjusted using the observed total ozone. With the previous procedure, the a priori profile varied from measurement to measurement, making it difficult to separate the contributions inherent in the measurements from those due strictly to the a priori information. The a priori in new updated UMK03 algorithm does not depend on total ozone, and therefore does not carry any total ozone trend information.

B.4. A priori error covariance matrix (S_x).

In the strict implementation of the maximum likelihood estimation method one should generate the a priori error covariance matrix using the same dataset that was used to generate the mean profiles. However, it has been noted by many authors [e.g., Mateer & DeLuisi, 1992] that this so-called climatological covariance matrix has unwanted properties, including the fact that such matrices are often found to be nearly singular. A more serious problem is that for techniques such as the Umkehr, where the main objective is to study inter-annual and long-term changes in ozone, rather than short-term variability, the covariance matrix should ideally represent year-to-year variability of monthly mean ozone rather than short-term variability. For these reasons we assume that the fractional uncertainty in the a priori is same in all layers and the correlation between layers falls off exponentially with layer number. This leads to the following form of the a priori error covariance:

$$\left[COV\left(\ln \omega\right)\right]_{ij} = C \times \exp\left(-\left[i-j\right]/k\right) \qquad \text{(B4)}$$

where, $C=Var(ln\omega)$ is the assumed variance (square of standard deviation) of ozone in all layers, and k is a smoothing parameter. In the X coordinate system, we get:

$$\left[COV\left(\omega\right)\right]_{ij} = C \times \omega_i \times \omega_j \exp\left(-\left[i-j\right]/k\right) \qquad \text{(B5)}$$

where ω_i is the ozone in the i-th layer of the a priori profile. In section 5.1 we describe our procedure for selecting the proper values of C and k.

B.5. First Guess (x_1).

For nearly linear problems, the inverse model (Eq. B2) should converge to the same profile, independent of the first guess (x_1). However, the retrieval can never be made independent of the a priori, x_0. Nevertheless, the first guess can be used to speed up the convergence in the inverse problem. The UMK03 algorithm uses standard ozone profiles for the first guess, MSC and Jacobian matrix tables.

The set of standard ozone profiles are latitude and total ozone dependent, and have been created to present typical ozone profile behavior at high, middle and low latitudes at the sea-level pressure (similar to standard profile used in the SBUV algorithm, V.8, McPeters, 1998). The total ozone column of standard profiles ranges between 125 and 575 DU in 50 DU increments. In order to correct the standard ozone profile for altitude of the station, first, ozone amounts in the tropospheric layer of standard ozone profiles are adjusted for the pressure of the station; thus, total ozone in standard profiles is altitude corrected. Then, altitude-adjusted standard profiles are linearly interpolated to the observed total ozone.

B.6. Measurement vector *($y_1(\theta)$).*

The measurement vector contains normalized N-values, $y_1(\theta) = N(\theta) - N(\theta_0)$ (see Eq. A2), where the size of the vector can vary from 11 to 7 parameters (depending upon the choice of the SZA for normalization). The measurement vector also includes total ozone information from direct sun measurement. We discuss the proper selection of $\boldsymbol{\theta_0}$ in section 5.2.

B.7. Measurement Error Covariance Matrix (S_e).

The UMK92 algorithm assumes that the standard deviation of Umkehr measurements at each solar zenith angle is 1 N-value, and that the errors between SZAs are uncorrelated. Thus, normalization increases the standard deviation to 1.4 N, leading to a diagonal measurement error covariance matrix, S_e, with 2 along the diagonal. Based on careful examination of the Umkehr data simultaneously collected from two automated Dobson instruments located at Arosa, Switzerland (Rene Stubi and Eliane Maillard, MeteoSwiss, private comm.) we believe that the measurement errors increase with SZA. Therefore, for automated Dobson measurements we recommend changing S_e (See Table B for diagonal elements, where 0.25 value assumes that the noise of normalized measurement is 0.5 N). The effect of the measurement noise on the retrieved ozone profile data is discussed in sections 6 and 7.2.1.

Appendix C. Definition of Averaging Kernel.

The ideal AK is a unity matrix, meaning that the system is capable of transferring independent layer information to an appropriate layer of the retrieved profile without interference from other layers and information loss. Numbers that are less than one indicate that not all information was transferred to the layer. Because the system is constrained to preserve total ozone value, the lost information has to be derived elsewhere. Most of the time, it is delivered to the adjoining layers. If the AKs have a Gaussian shape, the width of the Gaussian at the half-maximum point represents the resolution of the technique. However, if they are not Gaussian, interpreting the information content becomes trickier. For convenience, we rewrite Rodgers' AK formula to express layer-ozone changes in fraction of the a priori ozone, which gives:

$$\left(\omega_{RT}^{i}-\omega_{0}^{i}\right)\Big/\omega_{0}^{i}=AK_{ij}\times\omega_{0}^{j}\Big/\omega_{0}^{i}\times\left(\omega_{T}^{j}-\omega_{0}^{j}\right)\Big/\omega_{0}^{j} \qquad \text{(C1)}$$

Figure C shows the fractional AKs, i.e. $AK_{ij}*\omega_0^j/\omega_0^i$. The 61-layer AKs calculated for a typical middle latitude ozone profile show how the algorithm responds to a 1 percent ozone change in a layer of width dlogp=log2/4 (approx. 1.2 km). The numbers in the graph represent the altitude of the layer center at which the change is made. The plot shows that the response of the algorithm is to broaden the perturbation over many layers. It also shows that information at altitudes between 20 and 40 km is very similar. The AK at any altitude in this range can be described roughly as a Gaussian weighted distribution. The full width at half maximum of the response is about between 8 and 10 km. The plot also shows that the algorithm cannot separate a 40.2 km perturbation from the one at 46 km. (The higher altitudes are not shown but they also overlap with the 46 km response.) The ozone profile information contained in layers below 20 km presents a tougher problem. It is clear that the information in these layers is highly distorted with contributions coming from all levels. The AK depends somewhat on the vertical ozone distribution.

Table A. Second-degree polynomial fit coefficients for middle latitude ozone profiles (see Eq. A5).

SZA	A	B	C*100
60	51.08	0.17	-0.003
65	60.16	0.19	-0.005
70	72.86	0.22	-0.008
74	86.85	0.25	-0.015
77	100.21	0.26	-0.023
80	115.68	0.26	-0.033
83	130.60	0.22	-0.035
85	137.21	0.17	-0.025
86.5	138.83	0.13	-0.024
88	136.97	0.10	-0.005
89	133.77	0.10	-0.002
90	129.05	0.09	-0.000

Table B. Measurement error matrix, Se.

SZA	65	70	74	77	80	83	85	86.5	88	89	90	TO
Variance	0.15	0.15	0.15	0.20	0.25	0.30	0.35	0.40	0.70	1.40	2.80	0.1

Table 1. Umkehr layer system.

Layers	Layer Boundary (km)	Pressure limits (hPa)
0+1	0 - 10	1013 - 253
2+3	10 - 20	253 - 63
4	20 –25	63 – 32
5	25 - 30	32 –16
6	30 – 35	16 – 8
7	35 - 40	8 -4
8	40 - 45	4 - 2
9	45 -50	2 – 1
8+	40 – top of atmosphere	4 - 0

Table 2. Contribution Functions *Dn* (Appendix B, Eq. B3) for middle latitude 325 DU standard ozone profile as function of SZA (columns) and layers (rows).

Layer\SZA	60^0	65^0	70^0	74^0	77^0	80^0	83^0	85^0	86.5^0	88^0	89^0	90^0
9+	0.00	0.00	0.02	0.03	0.07	0.08	0.00	-0.11	-0.16	-0.03	-0.42	0.03
8	0.01	0.03	0.06	0.08	0.09	0.03	-0.07	-0.11	-0.02	0.16	0.37	0.14
7	0.05	0.09	0.10	0.04	-0.13	-0.30	-0.07	0.45	0.90	0.56	-0.94	0.59
6	-0.03	-0.13	-0.28	-0.44	-0.49	0.14	1.11	1.47	0.59	-0.62	-1.33	0.85
5	-0.22	-0.42	-0.40	-0.02	1.03	2.30	1.50	-0.59	-2.15	-1.31	1.27	-1.65
4	0.22	0.67	1.28	1.84	1.99	0.32	-1.71	-2.05	-0.53	0.65	1.02	-1.97
2+3	0.51	0.99	1.07	0.55	-0.88	-2.44	-1.60	0.20	1.28	0.83	-0.54	4.85
0+1	-0.19	-0.55	-1.01	-1.37	-1.40	-0.49	0.42	0.63	0.27	-0.08	-0.33	5.50

Table 3a. Change in 12 N-values due to stratospheric (0.1 optical depth) and tropospheric (0.3 optical depth) aerosols, for 350 DU standard ozone profile.

Type\SZA	60^0	65^0	70^0	74^0	77^0	80^0	83^0	85^0	86.5^0	88^0	89^0	90^0
STR, 10-km	0.9	0.8	0.6	0.4	0.3	0.1	-0.0	-0.1	-0.1	-0.0	0.1	0.3
STR, 15-km	1.0	0.8	0.4	0.0	-0.5	-1.0	-1.4	-1.5	-1.8	-2.3	-2.6	-2.5
STR, 20-km	1.0	0.5	-0.2	-1.4	-2.7	-4.4	-5.5	-5.1	-4.5	-4.7	-5.8	-7.4
STR, 25-km	0.6	-0.2	-1.8	-4.2	-7.4	-11.7	-15.4	-14.9	-12.3	-9.2	-9.0	-12.0
TROP, ABS	-0.4	-0.6	-0.8	-1.1	-1.4	-1.5	-1.3	-0.9	-0.7	-0.5	-0.5	-0.5
TROP, non-ABS	3.2	3.1	2.9	2.7	2.6	2.5	2.6	2.7	2.8	2.8	2.8	2.8

Table 3b. Change in 8 Umkehr layers (percent) corresponding changes to stratospheric (0.1) and tropospheric (OD of 0.3) aerosols, for 350 DU standard ozone profile.

Type\Layer	8+	8	7	6	5	4	2+3	0+1
STR, 10-km	-3.2	-3.9	-4.7	-3.2	-1.2	-0.9	0.3	3.0
STR, 15-km	-15.8	-17.7	-11.3	-1.5	-1.2	-4.1	1.1	7.8
STR, 20-km	-42.9	-46.0	-11.2	3.1	-19.3	-18.3	14.1	26.1
STR, 25-km	-67.5	-73.0	-7.5	-6.5	-58.0	-39.3	48.4	56.0
TROP, ABS	-3.5	-3.7	-1.6	-0.2	-3.1	-5.2	-0.5	6.0
TROP, NABS	-2.9	-3.0	-1.2	0.2	-1.3	-2.7	-0.2	3.2

Table 4. Error in MSC N-values due to 1 DU error in total ozone at the middle latitude.

error\SZA	60^0	65^0	70^0	74^0	77^0	80^0	83^0	85^0	86.5^0	88^0	89^0	90^0
dN*100	2.0	2.3	2.8	3.4	4.2	5.2	5.7	4.8	3.8	3.2	2.9	2.8

Table 5. The percent error in the retrieved ozone due to a priori information is shown for 8 individual layers, SD(RT-TR), without and with measurement noise error added.

	8+	8	7	6	5	4	2+3	1+0
Se(0.25), ***Sx***(0.1), no noise	1.6	3.1	2.7	3.9	4.3	8.1	10.7	11.6
Se(0.25), ***Sx***(0.1), with noise	4.1	4.5	5.7	5.2	6.0	9.0	11.6	13.7
Se(2.00), ***Sx***(0.1), with noise	6.8	7.0	6.1	7.3	6.9	10.6	15.2	13.8
Se(2.00), ***Sx***(0.4), with noise	9.2	8.7	9.6	8.8	9.6	12.3	14.0	17.4
Se(0.25), ***Sx***(0.1), monthly	1.4	1.9	2.2	2.5	2.7	4.1	5.8	6.5
Se(2.00), ***Sx***(0.4), monthly	3.4	3.3	3.4	3.6	3.8	5.3	6.6	7.8

Table 6. The percent error in the retrieved ozone due to the measurement noise.

	8+	8	7	6	5	4	2+3	1+0
Se(0.25), RT error for 325 DU	3.1	2.2	3.5	2.9	3.1	3.1	2.4	6.1
Se(2.00), RT error for 325 DU	4.3	3.6	3.6	4.6	4.0	2.7	4.0	6.7
Se(SZA), RT error for 325 DU	4.4	3.6	2.9	3.8	2.8	3.3	2.4	6.2

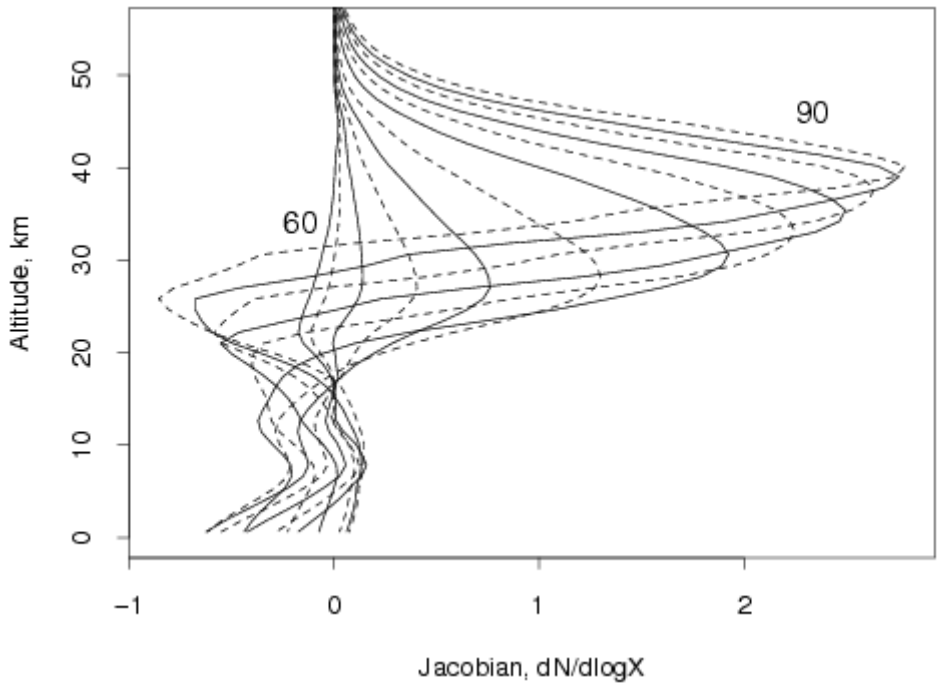

Figure A. Jacobian matrix dN/dnX is plotted as function of altitude and solar zenith angle. The N-value derivative at 60-degree SZA is shown as the first solid line from the left. The farthest dashed line to the right is the N-value derivative at 90-degrees SZA. Results at other SZA are shown as series of alternating dashed and solid lines located between 60 and 90-degrees. Results are shown for a standard middle latitude ozone profile with total ozone of 325 DU. The Jacobian matrix is normalized to total ozone.

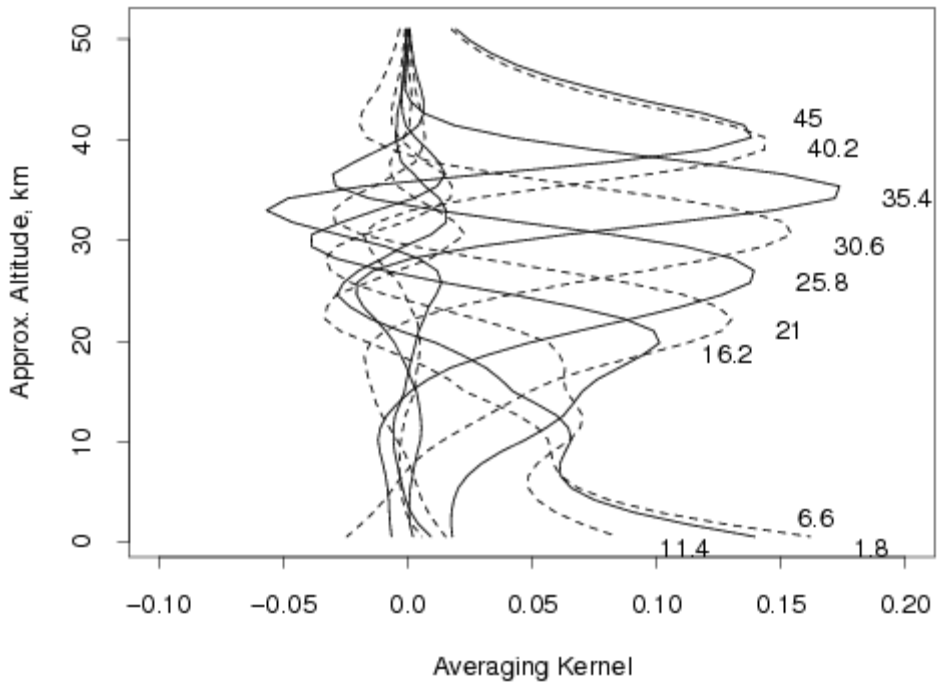

Figure C. Each line shows algorithm's response (AK) to a 1 percent ozone change in a thin layer (approximately 1.2 km wide) as function of altitude. The numbers in the graph represent the altitude of the layer center at which the perturbation is made. AK is for typical middle latitude ozone profile.

(a)

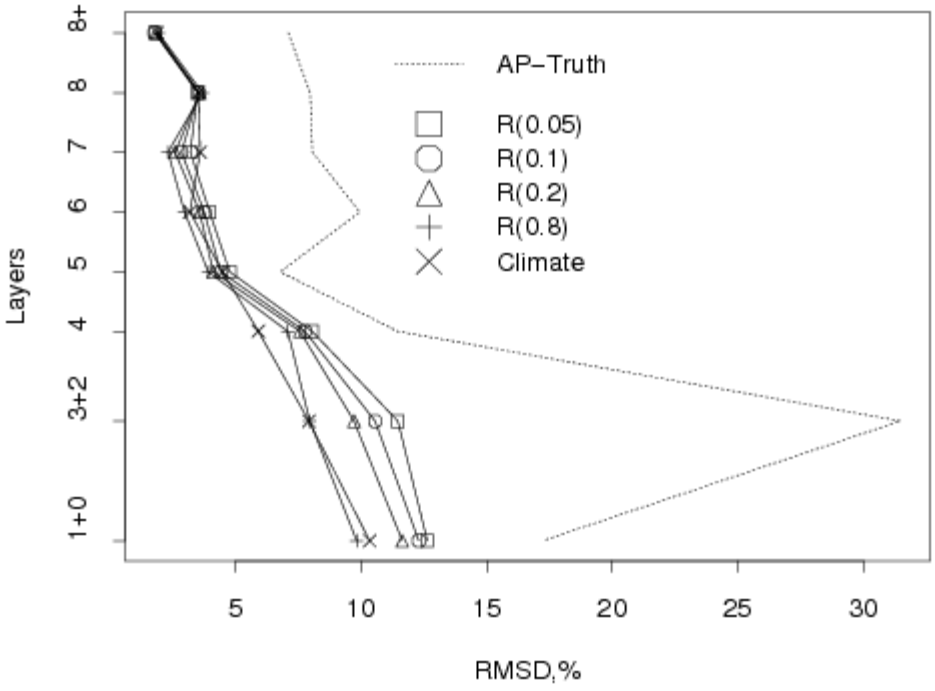

(b)

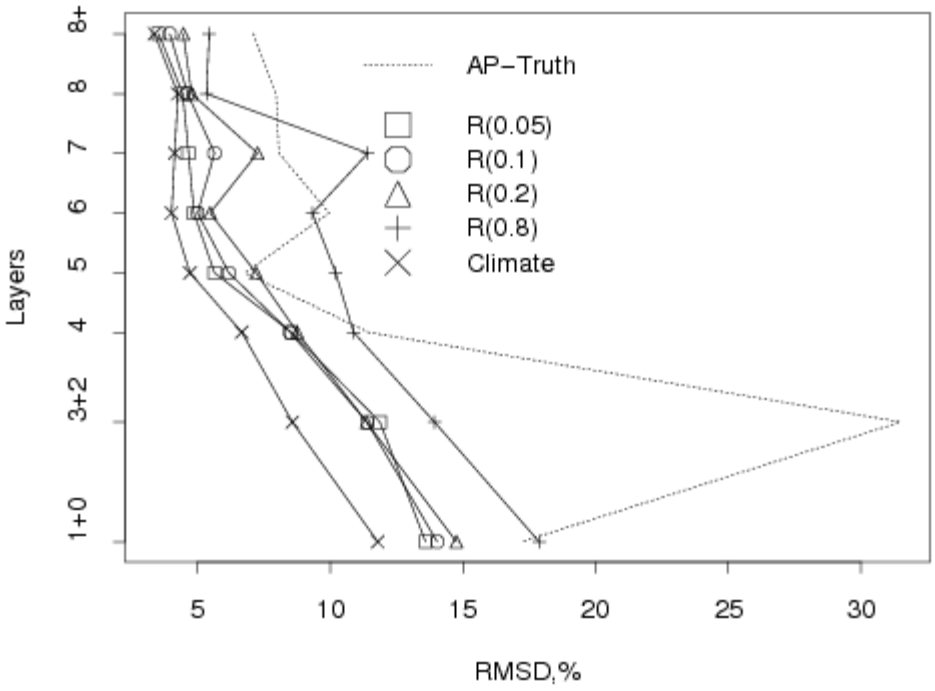

Figure 1. Standard deviation of the difference between the "truth" and the retrieved ozone profiles using a priori covariance matrices with different coefficients (indicated in legend). Results are given in percent relative to the mean synthetic ozone profile. The standard deviation (SD) of the difference between the "truth" and a priori profile, SD(AP-truth), is also given for reference. Results are given for the ozone profile retrieval based on synthesized Umkehr measurements either (a) without noise, or (b) with added random noise.

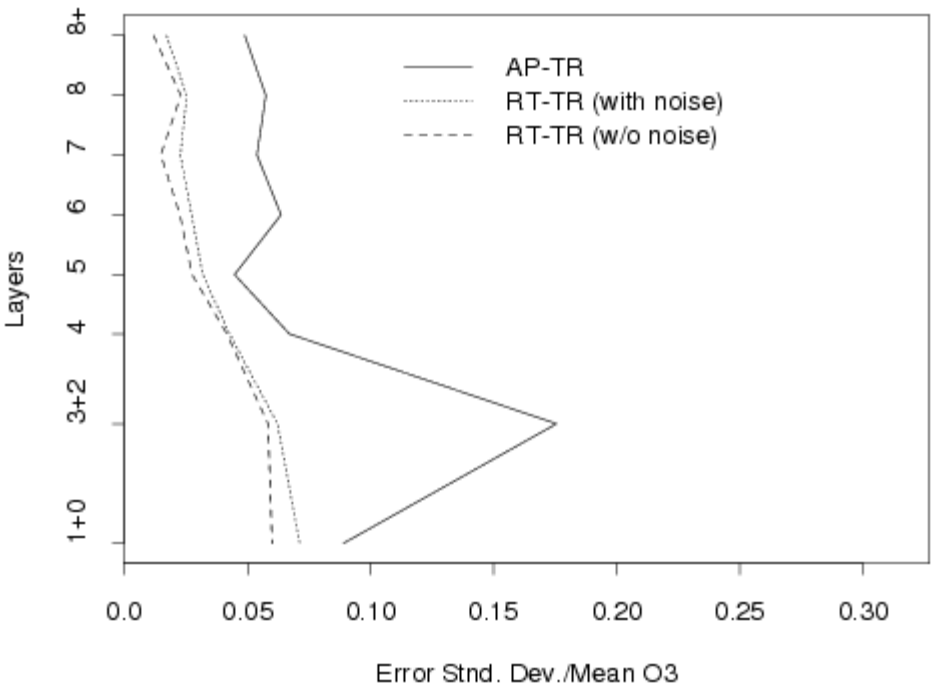

Figure 2. The standard deviation divided by mean ozone profile has been calculated for differences between the "a priori" ozone and the "truth"(solid line), as well as errors of the retrieval (dashed line) obtained with 60-degree SZA normalization (Xt, Xr, and Xap indicate truth, retrieved, and a priori ozone profiles respectively). The retrieval errors are also shown for a case when a random 0.5 N-value noise had been added to the synthesized N-values (dotted line). Errors are calculated for the monthly averaged data.

(a)

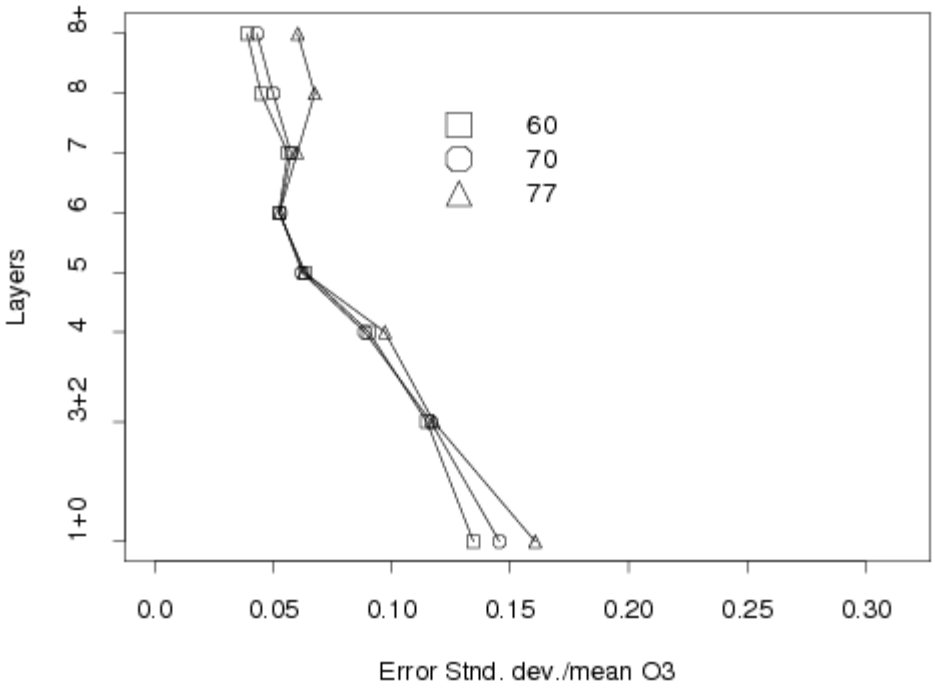

(b)

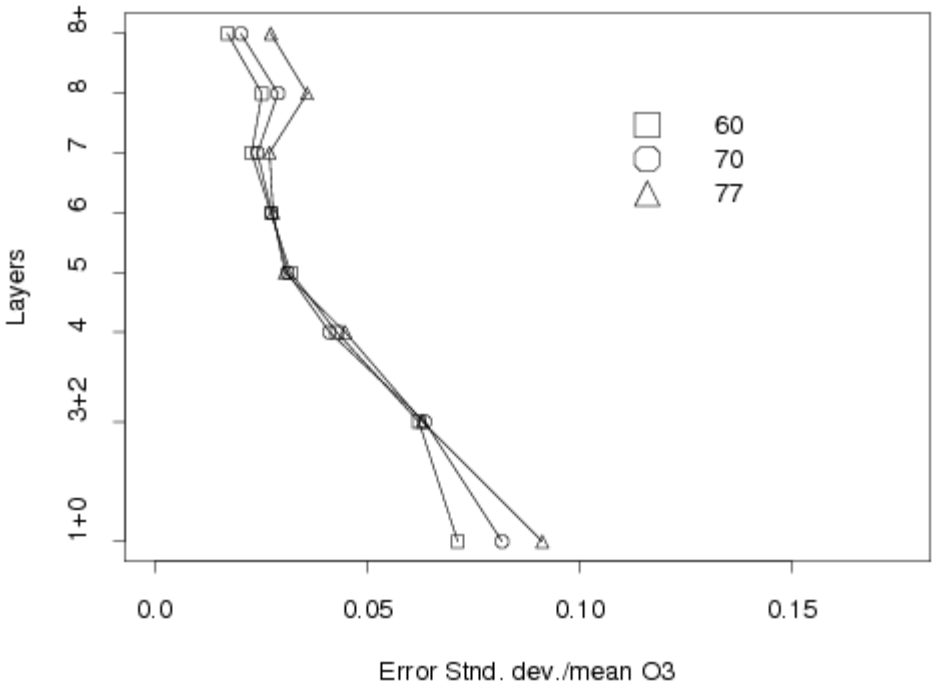

Figure 3. Relative error (standard deviation divided by mean ozone) of the retrieval as function of layers. The effect of the choice of the normalization SZA is shown by three lines representing three scenarios (60, 70 and 77 degree normalization SZA). (a) Reduction in daily errors, (b) Reduction in errors for monthly averaged retrievals with added random noise.

(a)

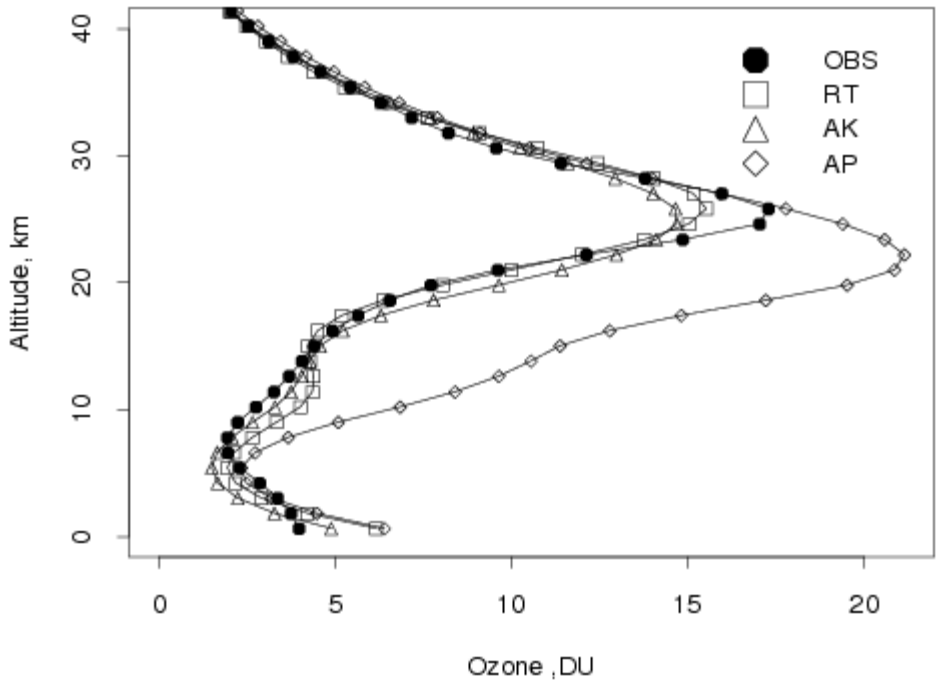

(b)

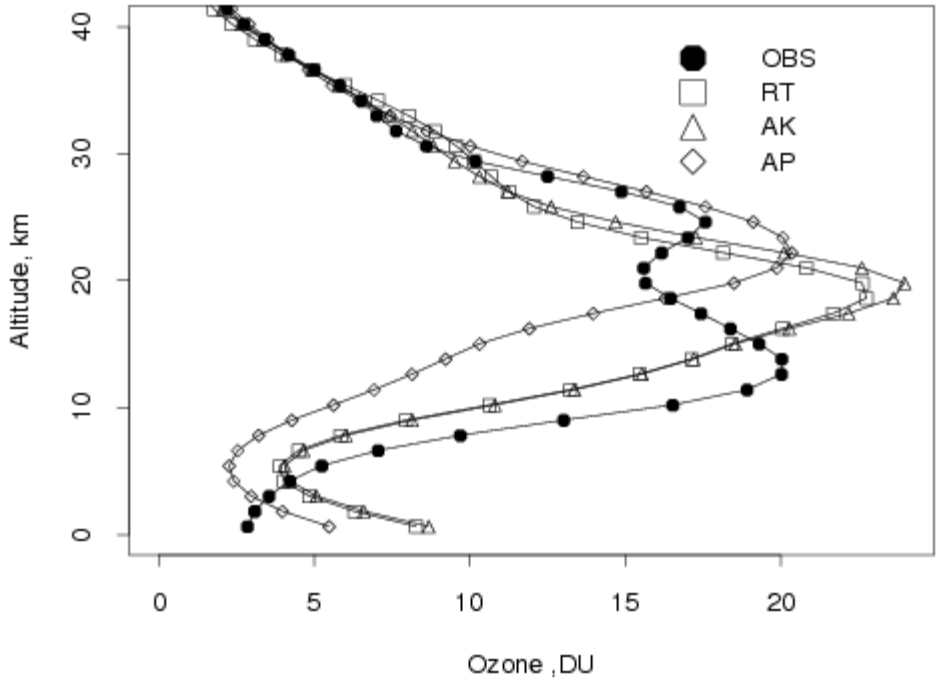

Figure 4. Comparisons of selected retrieved (RT) and test (OBS) ozone profiles in 61-layers. The a priori profile (AP) used for retrieval and profile obtained by using AK to smooth the referred test profile (AK) are also included for comparisons.(a) Smooth profile retrieval; (b) Perturbed profile retrieval.

(a)

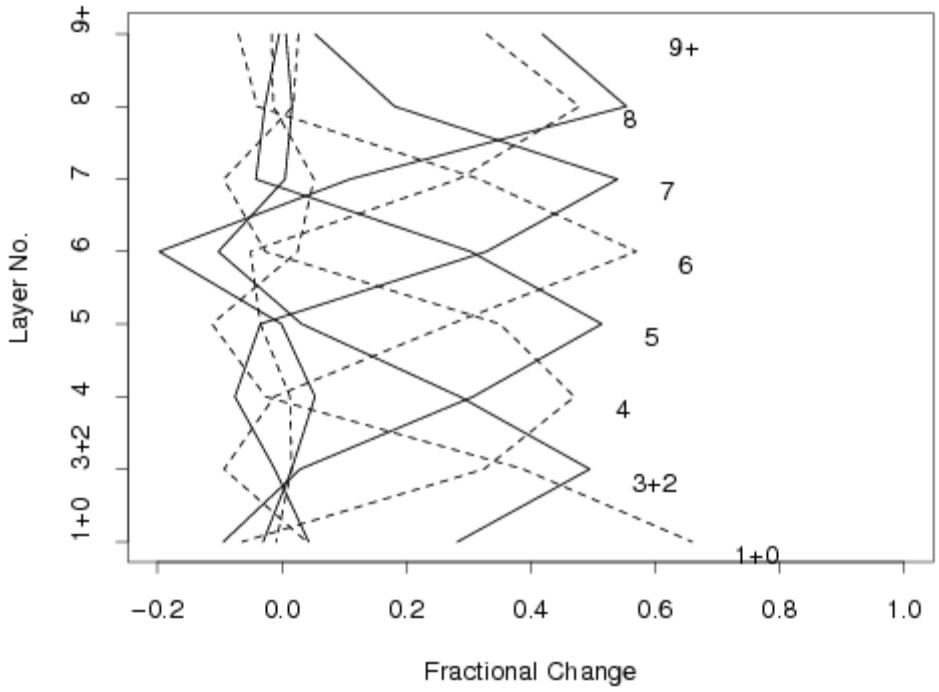
Layer No.
9+
8
7
6
5
4
3+2
1+0
−0.2
0.0
0.2
0.4
0.6
0.8
1.0
Fractional Change

(b)

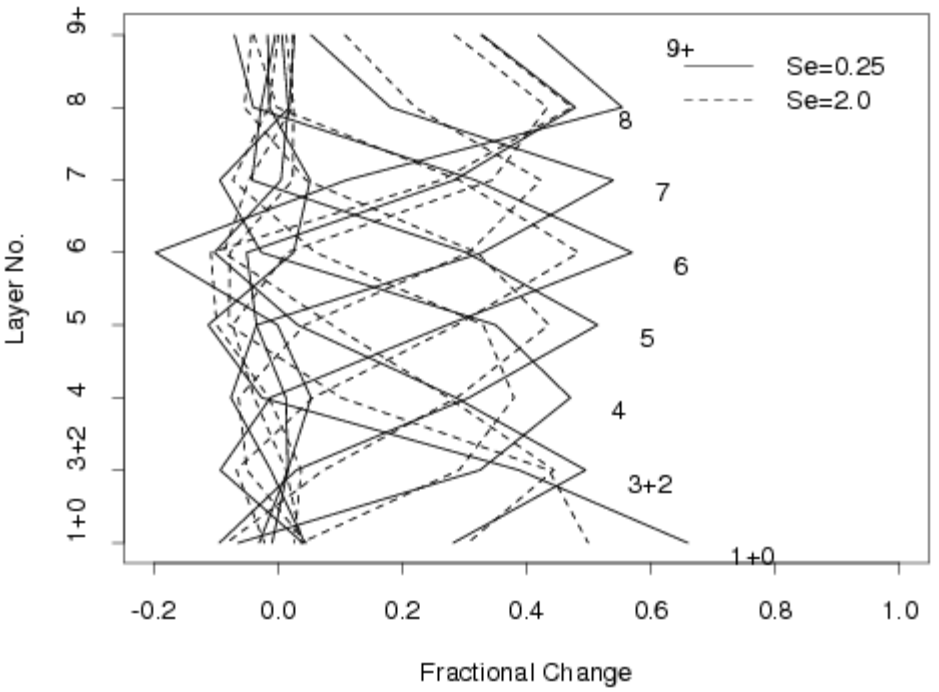
Layer No.
9+
8
7
6
5
4
3+2
1+0
Se=0.25
Se=2.0
-0.2
0.0
0.2
0.4
0.6
0.8
1.0
Fractional Change

(c)

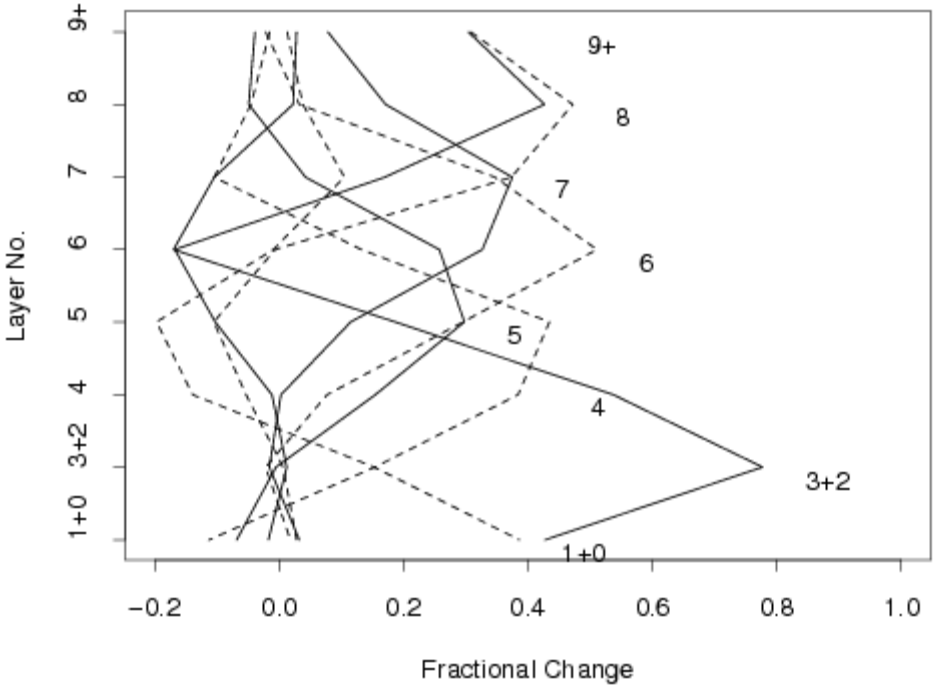

Figure 5. The same as Figure 2, but in 8 coarser layers (see Table 1 for details on layer system. (a) AKs are calculated using Rodgers covariance matrix with 0.2 coefficient and 60-degrees SZA for normalization. (b) The same as (a), but using two types of Se matrix representing lower (0.25) and higher (2.0) measurement noise; (c) The same as (a), but using climatological information about covariance between layers.

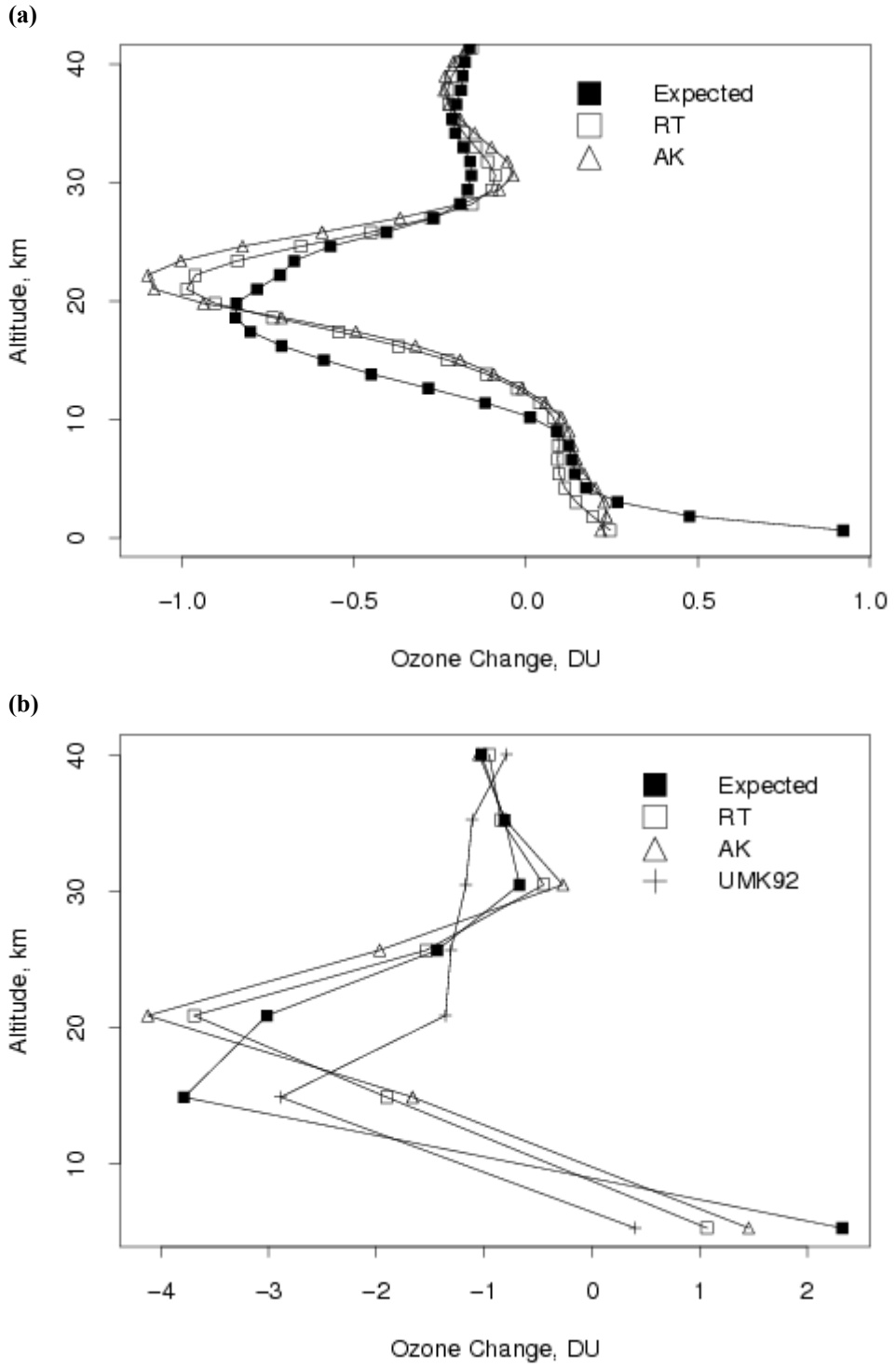

Figure 6. A vertical distribution of ozone profile changes (in DU per decade). The estimated trend in the ozone profile (sold squares) is compared with results of the new updated UMK03 algorithm (FAP) retrieval (open squares). The trend predicted using the method of Averaging Kernels (AK) is also shown (open circles). (a) Highly resolved vertical profile change in 61-layers. (b) The same as (a), but in 8 coarser layers. Results of the UMK92 algorithm (TOAP) retrieval (open triangles) are also included for reference.